Aus der Klinik und Poliklinik für Augenheilkunde

der Universität Würzburg

Direktor: Professor Dr. med. Jost Hillenkamp

Trabeculopuncture as Predictive Test for the Outcome of Ab Interno Trabeculectomy in Porcine Anterior Segments

Inauguraldissertation

zur Erlangung der Doktorwürde der

Medizinischen Fakultät

der

Julius-Maximilians-Universität Würzburg

vorgelegt von

Raoul Verma-Führing

aus Würzburg

Würzburg, Oktober 2021

Referent bzw. Referentin: Prof. Dr. Nils Loewen

Korreferent bzw. Korreferentin: PD Dr. med. Winfried Göbel

Dekan: Prof. Dr. Matthias Frosch

Tag der mündlichen Prüfung: 27.07.2022

Der Promovend ist Arzt.

Table of Contents

Abstract

Aim: To investigate trabeculopuncture (TP) for predicting the outcome of ab interno trabeculectomy (AIT). AIT is an effective, low-risk procedure for open-angle glaucoma. It has a high use rate but fails in patients with an unidentified distal outflow resistance.

Methods: We bisected 81 enucleated porcine eyes and perfused them at a constant rate of 6 µl/min for 72 hours. They were assigned to two groups: trial (n=42) and control (n=39). Intraocular pressure (IOP) was measured continuously. At 24 hours, 4 YAG-laser trabeculopunctures on the nasal trabecular meshwork were performed, followed by a 180° AIT at the same site at 48 hours. Eyes were divided into TP and AIT responders and non-responders; the proportion of TP responders between both AIT groups was compared.

Results: Post-TP and post-AIT IOPs were lower than baseline IOP ($p=0.015$ and $p<0.01$, respectively). The success rates of TP and AIT were 69% and 85.7%, respectively. The proportion of TP responders among AIT responders was greater than that of AIT non-responders ($p<0.01$). The sensitivity and specificity of TP as a predictive test for AIT success were 77.7% and 83.3%, respectively. The positive and negative predictive values were 96.6% and 38.5%, respectively.

Conclusion: A 10% reduction in IOP after TP can be used to predict the success (>20% IOP decrease) of nasal 180° AIT in porcine eyes. As porcine eyes share many similarities with human eyes, our findings may have implications on the validity of this test as a predictor for surgical outcomes of AITs in humans.

1. Introduction

Epidemiology and Definition of Glaucoma

Glaucoma is a progressive optic nerve neuropathy associated with consecutive visual field defects and, therefore, potentially results in blindness [1]. A study by Quigley et al. in 2006 estimates the prevalence of Glaucoma for 2020 is one of the most quoted ophthalmological studies to date [2]. This fact demonstrates the consistently high relevance of Glaucoma research and the yet unsaturated need of expanding the current literature. Glaucoma is the second most common leading cause of blindness after lens opacification (cataract) and is still on the rise. Quigley et al. estimated the prevalence in 2020 to be approximately 80 million, representing about 1% of the world's population. More recent findings by Allison et al. support these figures and estimate an increase to over 100 million glaucoma patients in 2040 [3]. It is assumed that almost half of all those people diseased with glaucoma do not know about their condition [4]. One reason for this is that glaucoma is a slowly progressing condition that can be asymptomatic until the moderate stages of the disease [5]. Another reason is the lack of adequate screening programs, especially in developing countries, and regular follow-ups of diagnosed patients [6]. Hence, it is essential to identify predispositions, drugs, and conditions that increase the likelihood of glaucoma development [7]. Among identifiable risk factors for glaucoma are advanced age, a positive family history, diabetes or cardiovascular diseases, and African American, Asian, or Hispanic descent [8]. All of these risk factors are currently on the rise. The global population's continuous growth and average life expectancy are expected to increase, and thereby the incidence of glaucoma [3,9]. Additionally, diabetes and cardiovascular diseases are likewise on the rise, potentially contributing to the increase in glaucoma patients [10–12]. Therefore, the necessity of detection and the demand for new treatment options are high, and current glaucoma practices are constantly required. Nevertheless, there is no cure for this disease, despite many research efforts.

Pathophysiology of Glaucoma

The pathophysiology of glaucoma is not fully understood yet; an increased intraocular pressure (IOP) is regarded as the most critical risk factor [13]. The physiological IOP ranges from 10-21 mmHg with a mean IOP of 15.5 mmHg [14] determined by an equilibrium of aqueous humor (AH) in- and outflow in the eye. AH is formed at approximately 2.5 µL/min by the ciliary body epithelium [15]. AH flows around

the iris from the eye's posterior chamber through the pupil into the anterior chamber. There, AH drains into the outflow tract through the trabecular meshwork (conventional outflow) and the uveoscleral tissue (unconventional outflow) [15]. Figure 1 depicts the circulation of AH in the eye. Increased IOP levels lead to irreversible damage of the ganglion cell axons in the retinal nerve fiber layer (RNFL). All axons run, bundled as the optic nerve to the optic chiasm where the optic fibers partially cross and are henceforth named optic tract. The fibers from the optic tract eventually end in the visual cortex. Nerve fibers of the peripheral retina are located at the outer regions of the optic nerve; fibers of the central retina are at the inner regions. As the most stress by an elevated IOP is exerted on the inferotemporal and superotemporal axons, corresponding superonasal and inferonasal steps in the visual field are the most common early functional defects [16,17]. The disease progresses most of the time slowly, and patients do not experience pain unless severely elevated IOP levels arise.

Figure 1 Aqueous Humor Circulation

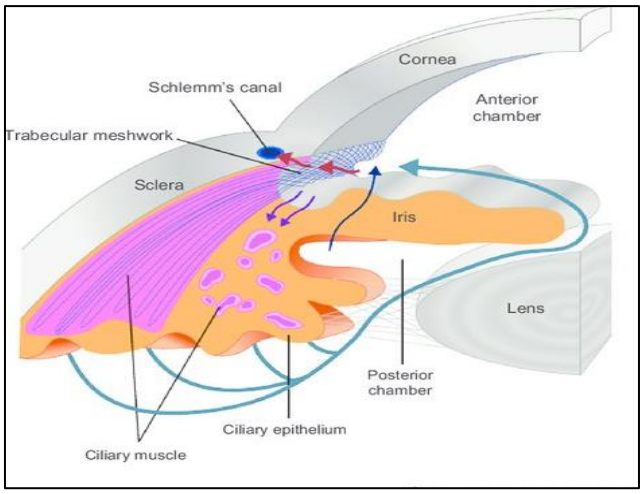

Figure 1 depicts the flow of aqueous humor from the posterior to the anterior chamber of the eye (blue arrow).[18] It is produced by the ciliary processes, then flows around the iris into the anterior chamber, and eventually drains through the outflow tract into the episcleral veins (red arrows).

Out of both outflow pathways, only the conventional outflow system is pressure-dependent, permitting more flow with increased IOP. It can be subdivided into proximal and distal portions [19]. The trabecular meshwork (TM) represents the proximal part of the conventional outflow tract and can be visualized by gonioscopy during a clinical examination. Figure 2A depicts a gonioscopic view of an open anterior chamber angle. It is a porous region that can be subdivided into different cell layers: the uveal meshwork, corneoscleral meshwork, juxtacanalicular meshwork, and inner wall endothelium of Schlemm's canal (SC) (Figure 2B). AH passes through the TM, the inner wall of SC, and eventually enters SC. From here, the distal outflow starts by the

AH draining into collector channels through their proximal openings, into the meandering deep scleral plexus, and finally entering the episcleral veins [20,21].

Figure 2 Structure of the Trabecular Meshwork

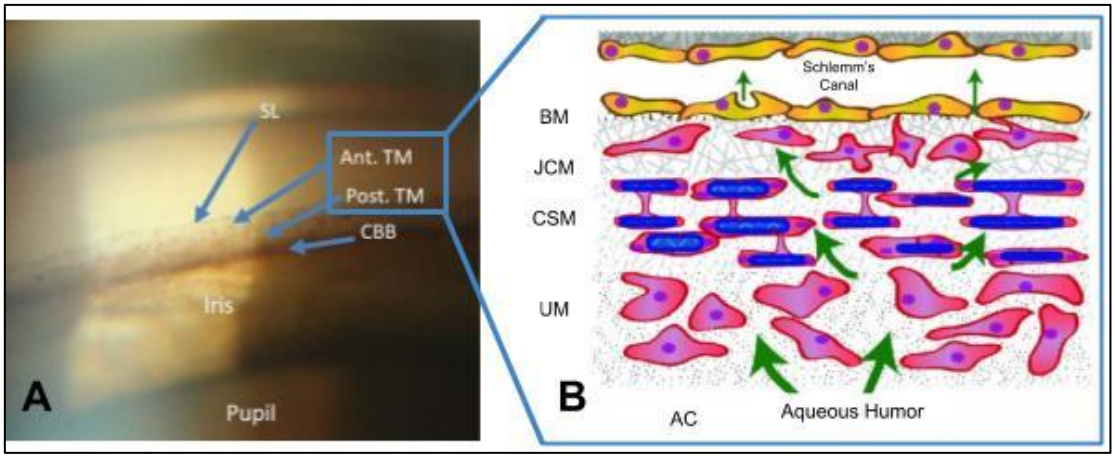

Figure 2A shows the structures of the anterior chamber on a gonioscopic view.[22] The trabecular meshwork is located between Schwalbe's line and the scleral spur. On the right side (2B), the structure of the trabecular meshwork is depicted.[23] The green arrows indicate the flow of aqueous humor from the anterior chamber into Schlemm's canal.
AC = anterior chamber; Ant. TM = anterior trabecular meshwork; BM = basement membrane; CCB = ciliary body band; CSM = corneoscleral meshwork; JCM = juxtacanalicular meshwork; Post. TM = posterior trabecular meshwork; SL = Schwalbe's line; UM = uveal meshwork

The uveoscleral outflow system is a pressure-independent outflow system that absorbs aqueous through the iris, ciliary body, ciliary body band, and other, more posterior parts of the uvea. Only the conventional outflow system can be surgically modified. Goldmann's equation describes the relationship between IOP and the outflow facility that is reciprocal to the outflow facility [20]. Thus, outflow (A) is equal to the aqueous formation (F) and can be expressed as the quotient of pressure (P) and outflow resistance (W).

$$A = P / W$$

Given that outflow resistance is the reciprocal of outflow facility (C)

$$C = 1/W$$

and the gradient that drives outflow is the difference between IOP and episcleral venous pressure (EVP), one obtains:

$$F = (IOP - EVP) * C$$

This equation is known as the Goldmann equation. Accordingly, an increase in outflow facility leads to a reduction of IOP under the assumption that F and P_e remain unchanged. By implication, elevated IOP levels are induced by either an imbalance of formation and outflow of AH or an increased outflow resistance. As the formation of AH decreases with age, in the majority of glaucomas the most likely cause of a raised IOP is increased resistance to outflow [21,24]. Blockage of the TM for instance can occur through primary and secondary angle-closure by the iris, adhesions (synechiae), or proliferative membranes. Furthermore, debris, fibrillary material, or pigment can obstruct the TM and increase the outflow resistance. However, in the absence of these pathological conditions the main site of physiological outflow resistance lies in the tightest layers: juxtacanalicular meshwork and the inner wall of SC [21,25]. The distal outflow facility is determined by the lumen of the vessels as well as the EVP. It has been shown to contribute to approximately 25-50% of the total outflow resistance [26]. Narrowing of the SC lumen by a transient increase in IOP can lead to herniations at the ostia of the collector channels, causing a decrease in the outflow facility [27,28]. An elevated EVP is defined as pressure above 8 mmHg. The condition can be found in various conditions, ranging from arteriovenous shunts to ocular tumors [20,29]. As a consequence of an increased EVP, blood reflux into SC occurs which impedes AH drainage into the outflow tract and subsequently leads to a rise in IOP [30,31].

Types of Glaucoma

Glaucoma can be subdivided into primary and secondary entities that can further be subset into different subtypes. Primary glaucomas are classified by the opening of the anterior chamber angle as primary open-angle glaucoma (POAG) and primary angle-closure glaucoma. POAG is the most common glaucoma type in the western hemisphere, with a prevalence of about 2% and 4% in the Caucasian and African American population, respectively; primary angle-closure glaucoma has its highest prevalence in Asia with 0.7%. [3,20,32,33]

In POAG, despite a normal appearance of the angle on gonioscopy, progressive damage to the optic nerve is causing irreversible visual field defects. Retinal ganglion cells and axons decay and result in pathognomonic cupping of the optic nerve head. An elevated IOP caused by a decrease in outflow facility is often the most important risk factor [20]. However, the exact etiology is still unclear and there are also individuals with an open angle and low IOP showing likewise signs of glaucoma. In this case, they are referred to low tension glaucoma patients [20].

Secondary glaucomas include pseudoexfoliation, pigmentary, uveitic, and neovascular glaucoma. Exfoliation material is fibrillary deposits that accumulate in the TM and consecutively decrease the outflow facility. In pigmentary glaucoma, pigment derives through friction from the posterior iris epithelium and likewise obstructs the TM. Secondary angle-closure by fibrovascular membranes is the pathomechanism of neovascular glaucoma. These membranes develop on the ground of an underlying ocular or systemic disease, for instance, retinal vein occlusion or diabetes. In contrast to POAG, all these conditions share an identifiable mechanism for increased trabecular meshwork resistance and thus elevated IOP values [20,34].

Treatment of Glaucoma

IOP reduction is currently the only available treatment for glaucoma and falls into one of two categories: conservative and surgical. First-line therapy consists of either topical medication or selective laser trabeculoplasty (SLT). [35,36]

Today, the most commonly used anti-glaucomatous eye drops can be classified into one of 5 categories: beta-blockers, carbonic anhydrase inhibitors, alpha-2 adrenergic agonists, prostaglandin analogs, and Rho kinase inhibitors [20,37]. While the first three mainly modulate the formation of AH by the ciliary body, the latter two increase AH outflow through the uveoscleral and trabecular pathways, respectively [37–39].

Laser Treatments for Glaucoma

Laser trabeculoplasty on the TM can be performed as an alternative treatment or in addition to topical therapy. SLT was introduced in 1995 and is a minimally invasive laser treatment intended to increase the conventional AH outflow by cellular modulation of the TM [36]. A Q-switched neodymium-doped yttrium aluminum garnet (Nd:YAG) laser at a wavelength of approximately 532 nm is deployed to perform a 90° — 360° trabeculoplasty in single shots of 0.9 – 1.1 mJ per shot [40]. Melanin located in the TM absorbs light at a wavelength of 400-700 nm [41]; consequently, thermal energy is selectively absorbed by these pigmented TM cells at the spot of pulsation [42]. As the deployed energy level is low, and the spot size is large (400 µm), there is no substantial coagulative damage to the surrounding tissue [43,44]. SLT is presumed to increase the outflow facility by the biological response of TM cells [44].

While the precise mechanism of action is not completely understood yet, clinical trials have shown SLT to be equal to drops as an initial treatment for glaucoma [36].

The IOP lowering effect of SLT is seldom permanent [45]; however, the procedure can be repeatedly performed [46]. The predecessor of SLT, Argon laser trabeculoplasty (ALT), was first described in 1979 [42,47]. For ALT, a blue-green laser is deployed [48]. The target of the electromagnetic laser energy is also the melanin localized in the TM. Similar to SLT, one theory regarding the mechanism of action of ALT assumes a remodeling of the TM. In contrast to SLT, another theory attributes the IOP lowering effect of ALT to contraction due to scarring of the treated spots that lead to a dilation of the adjacent TM regions [49]. Even though ALT and SLT have been shown to be similar regarding IOP reduction, the better risk profile, a lower amount of energy used, and easy handling have led to a wider establishment of SLT [36].

Trabeculectomy

Although first-line treatment options (SLT and drops) may achieve desired IOP levels in some patients, about 50% of glaucoma patients will eventually require at least one surgery [50]. Traditional glaucoma filtering surgeries are aimed at lowering the IOP sufficiently by bypassing the TM and creating a secondary outflow tract [51]. However, these interventions are associated with a high rate of post-surgical complications and require intensive postoperative care [52,53].

Trabeculectomy is indicated in uncontrolled or progressing glaucoma of patients on maximal topical therapy and insufficient response to laser therapy. IOP reduction is achieved by creating an additional outflow tract through a fistula.[37] Figure 3 depicts the newly created drainage pathway from the anterior chamber into the subconjunctival space through a scleral flap. A bleb will form on account of this newly created pathway into the subconjunctival space. Trabeculectomy success depends on intensive postoperative care and is often hampered by a high complication and failure rate of up to 60% and 40%, respectively [54,55]. More recent methods of filtering surgery deploy microshunts [56] or gel stents [57] for a safer approach [58,59]. Nevertheless, even those modern techniques are still associated with unfavorable postoperative adverse events such as a flat anterior chamber, choroidal effusion, hypotony, and deterioration of the visual acuity [56,60]. Due to the high complication rate, intensive postoperative care is required and furthermore, additional treatment with subconjunctival 5-Fluorouracil injections within the first postoperative days may also be indicated [53,61].

Figure 3 New Drainage Pathway after Trabeculectomy

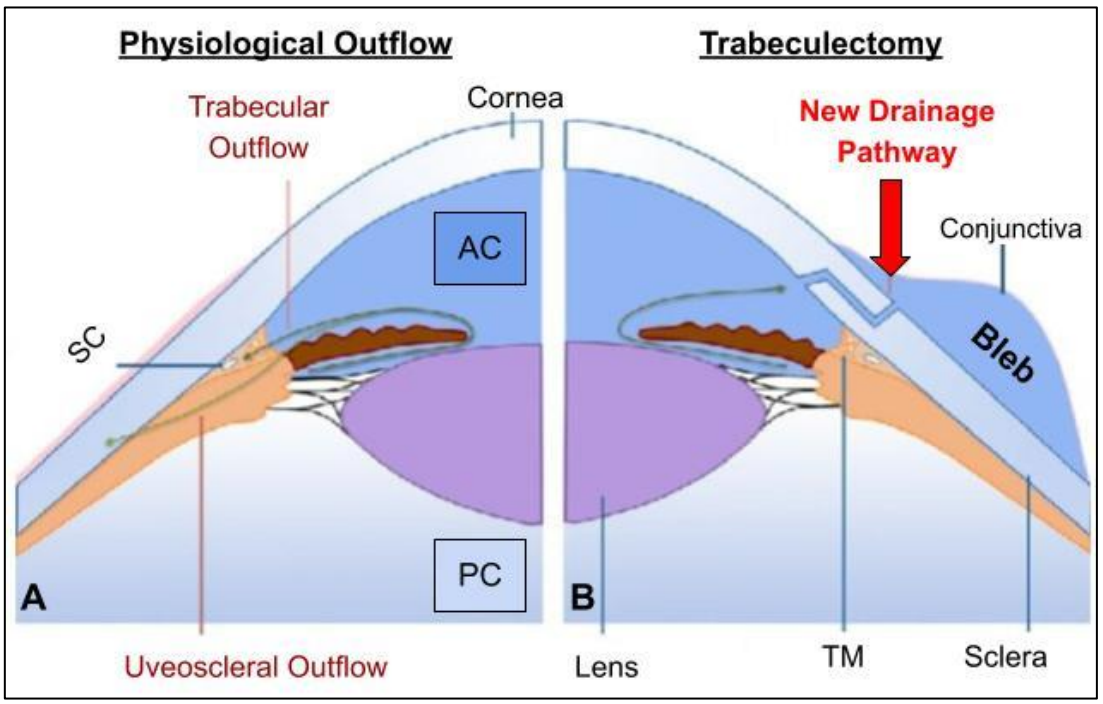

Figure 3 displays the newly created drainage pathway after trabeculectomy (B). In addition to the conventional outflow through the trabecular meshwork (A), aqueous humor now also drains through a scleral flap into the subconjunctival space and forms a bleb. [62]
AC = anterior chamber; PC = posterior chamber; SC = Schlemm's Canal; TM = trabecular meshwork

Microinvasive Glaucoma Surgery (MIGS)

To reduce surgical complications and costs, there has been a trend towards microinvasive glaucoma surgery (MIGS) over the last few decades. MIGS lower the IOP by removal or bypass of the TM and thereby enhance the aqueous humor outflow facility. [63,64] Moreover, they can serve as an alternative for glaucoma drops in case of intolerance or noncompliance and are even more cost-effective than topical treatment [65].

Trabecular micro-bypass stents are one type of MIGS that can circumvent the TM by draining the aqueous humor directly into the Schlemm's canal [64,66]. In 2012, the first generation of micro-bypass stents (iStent, Glaukos Corporation, San Clemente, California, United States) was approved by the United States Food and Drug Administration; in 2018 the second generation (iStent inject) was released. The first generation stent measured about 1 mm in length and 0.3 mm in height, the iStent inject presented a different shape and measured approximately 0.2 mm in length and 0.3 mm in height [67]. Figure 4 illustrates the first and second generations of iStents. The

implantation of 1-2 stents is usually performed in combination with cataract surgery [68]. This combined procedure has been shown to lower the IOP and the number of eye drops [66,69]. Phacoemulsification itself has been shown to be accompanied by a significant IOP reduction of about 2-3 mmHg [70,71]. Additionally, an increase in the outflow facility of the conventional pathway by TM bypass is assumed to contribute to the IOP reduction [66]. A 2020 meta-analysis by Chen et al. supports the effect of standalone stent implantation in lowering the IOP [72].

Figure 4 Trabecular Micro-Bypass Stent (iStent)

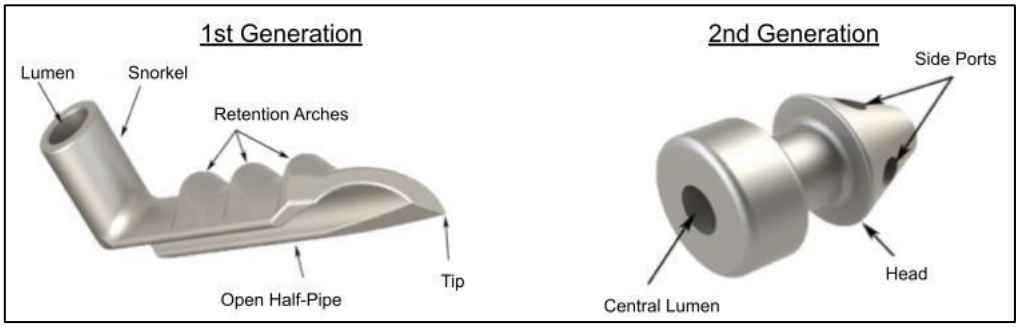

Figure 4 depicts the first and second generation of iStents. Both aim to enhance the conventional outflow by bypassing the trabecular meshwork.[73]

Another well-established MIGS is the deployment of various ab interno trabeculectomy (AIT) devices to either ablate [74], incise [75], or excise [76,77] the TM. As a consequence, the partial removal of the TM as proximal outflow resistance results in an IOP decrease. Owing to the surgical approach from the patient's temporal side, the nasal TM is the treatment area of most AIT devices [78]. For visualization of the anterior chamber angle structures, AIT requires the constant use of a surgical gonioscopy lens intraoperatively [78].

The Trabectome (MicroSurgical Technology, Redmond, WA, United States) is an anterior chamber maintaining AIT device that utilizes plasma-mediated ionization and disintegration for TM removal [79]. In Trabectome surgery, the tip of the handpiece is inserted into the anterior chamber and up to 180° of the nasal TM circumference are ablated, resulting in a theoretically complete elimination of proximal resistance at the treated site [78,79]. A footplate at the end of the tip prevents the surgeon from incising the outer wall of SC. Additionally, the device is equipped with an active irrigation and aspiration unit to maintain the anterior chamber during the intervention [80].

Similar to the Trabectome, the TrabEx (MicroSurgical Technology, Redmond, WA, United States) also allows active anterior chamber management during AIT. This dual-blade AIT device excises, rather than ablates, the TM [80]. Additionally, it allows the collection of TM samples [77]. However, the handling of the device is quite similar to that of the Trabectome. For MIGS devices without irrigation and aspiration, passive anterior chamber management by viscous substances is required [80]. One example is the Kahook Dual Blade, a goniotome that excises the TM similarly to the TrabEx [81]. Figure 5 depicts two of the above-mentioned trabeculectomy devices, the Trabectome and Kahook Dual Blade. They similarly succeed in reducing the proximal outflow resistance and thus lowering the IOP [82,83]. Additionally, they share a low-risk profile and quick rehabilitation after surgery. Success is commonly defined as 20% IOP reduction from baseline IOP and achieved in the majority of patients [84,85]. However, even after sufficient removal of the trabecular meshwork, approximately 30% of patients show an insufficient IOP reduction[86,87]. Furthermore, the average IOP after AIT in POAG patients is approximately 15 mmHg and not closer to the episcleral venous pressure of 8-10 mmHg [86,87]. Increased post-trabecular resistance is suspected to be the underlying reason for this effect, as well as the cause of AIT failure. Therefore, AIT is generally indicated for patients with mild to moderate glaucoma and targets IOP levels of around 15 mmHg [88].

Figure 5 Ab Interno Trabeculectomy Devices

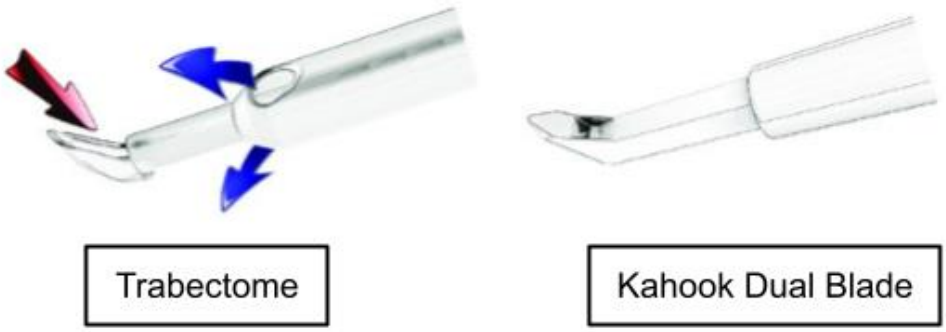

Figure 5 shows the tips of three different ab interno trabeculectomy devices. The Trabectome (left) uses plasma-mediated ionization to remove the trabecular meshwork (TM). The Kahook Dual Blade (middle) and TrabEx+ (right) excise the TM. The tips are inserted through a corneal incision into the anterior chamber. [80]

Cost Calculation

After the failure of AIT, a traditional filtering surgery (trabeculectomy) or a glaucoma drainage device is required. However, both have a significantly higher risk of serious complications and subsequent surgeries. If the probability of success could be determined beforehand, the surgical risk can be much reduced and unnecessary procedures can be avoided. The target IOP at which glaucoma stops progressing would be achieved sooner and there would be fewer sick days.

There will be decreased costs from fewer procedures, fewer hospitalizations, and fewer patient visits. In Germany, the annual treatment cost per glaucoma patient ranges from 918 € - 1194 €, depending on the severity of glaucoma[89]. The prevalence of OAG in Germany among adults aged 40 to 80 years old is about 2.51% [32,90]. This implies that the estimated total cost of glaucoma treatment in Germany is about 875 MM € per year (35 MM Germans between 40 – 80 years of age, prevalence 2.5%, the average cost of 1000 € per patient per year). The average cost for a standard glaucoma procedure in local anesthesia is about 2800 € according to Diagnosis Related Groups (C06Z G-DRG). In 2019, over 10,000 AIT or equivalent procedures were performed [91]. A one-year success rate of 70% leads to 3000 unsuccessful interventions. Consequently, a predictive test could save about 8.5 MM € annually by avoiding 2800 € for 3000 redundant interventions and their complications. So far, there is no such test to estimate the post-trabecular resistance and thus, predict the outcome of AIT. However, a minimally invasive procedure that could potentially aid in creating this much-needed predictive test might be trabeculopuncture (TP) with a Nd:YAG laser.

Trabeculopuncture

The idea of creating micropunctures in the TM to enhance the outflow facility was first introduced in the 1970s by the Russian ophthalmologist Mikhail Krasnov [92,93]. Before AIT until the early 90s, glaucoma specialists used lasers, such as argon-ion, ruby, or neodymium-doped yttrium aluminum garnet (Nd:YAG) to create these small punctures. The idea was to penetrate SC and thereby reduce the outflow resistance through the anterior portion of the TM. A mechanism, similar to that of trabecular-bypass stents [92]. Rassow et al. have shown a spot size of about 100 µm in diameter to create an adequate outflow [94]. Yet, an optimal spot size has not been established. In general, more than one puncture was performed to reduce the rate of

failure. Also, the applied laser energy levels differed among surgeons (Table 2). Mostly, moderate to high-energy levels were used for TP with the Nd:YAG laser.

TP was easy to perform, well-tolerated, had no serious side effects, and lowered IOP temporarily but fell out of favor because the effect was short-lived, lasting weeks to months. Table 1 depicts historical IOP outcomes of prior research on TP in human eyes; Table 2 summarizes the energy levels and laser settings deployed for TP. In 1973, Krasnov pioneered in using different types of lasers to perform TP in individuals with therapy-refractive open-angle glaucoma, resulting in a successful albeit temporary reduction of IOP [92]. In the same year, Worthen and Wickham published results on determining laser energy levels for safe TP in non-glaucomatous rhesus monkey eyes with an argon-ion laser [95,96]. Applying this procedure to human eyes only induced temporary IOP reduction [97]. However, argon laser trabeculotomy only helped to delay incisional glaucoma surgery from three months to maximal two years [98]. In 1985 Epstein started to perform TP with a Nd:YAG laser with mixed results; while the IOP decreased in juvenile open-angle glaucoma, none was seen in POAG [99]. Subsequent studies showed a more effective reduction of IOP by this laser [100], however. In angle recession glaucoma, Nd:YAG laser trabeculopuncture was superior to argon laser trabeculoplasty [101], which in contrast to TP does not fully penetrate through the TM into SC. Documented side effects from TP were mostly anterior chamber flare and cells, mild hemorrhage, and IOP spikes [101,102]. However, they resolved after treatment or even resolved spontaneously.

Table 1 Historical Outcomes of Trabeculopuncture

Table 1 summarizes the historical intraocular pressure (IOP) outcomes of trabeculopuncture (TP) with different lasers. Even though a sufficient IOP reduction was quickly achieved in several cases (Time to Through), the pressure-lowering effect of TP was only transient. Nd:YAG = neodymium-doped yttrium aluminum garnet laser

Laser	Included Eyes	Pre TP (mmHg)	Post TP (mmHg)	Reduction (mmHg)	Time to Trough	Investigator/ Year
Q-Switched Ruby	10	32.4	23.8	8.6	1 week	Krasnov 1973 [92]
Argon	45	36	24	12	3 months	Wickham & Worthen 1979 [98]
Nd:YAG	10	25.5	20	5.5	24 hours	Epstein 1985 [99]
Nd:YAG	8	25.6	19.1	6.5	1 hour	Melamed 1987[102]
Nd:YAG	79	28.9	21.7	7.2	1 month	Del Priore 1988 [100]
Nd:YAG	18	31	15	16	1 – 12 months	Fukuchi 1993 [101]
Excimer	35	-	-	7	-	Vogel 1997[103]
Excimer	28	25.3	16.5	8.8	-	Töteberg-Harms 2011[104]

Table 2 Historical Laser Settings for Trabeculopuncture

Table 2 shows the number of spots and laser settings of previous studies. The table highlights the inconsistent settings used for trabeculopuncture.
Nd:YAG = neodymium-doped yttrium aluminum garnet laser

Laser	Spots	Spot size	Energy	Duration	Investigator/ Year
Q-Switched Ruby	-	250-500 µm	0.2 J	-	Krasnov 1973 [92]
Argon	50	100 µm	1-3 W	0.1 s	Ticho 1978 [105]
Argon	100-150	50 µm	2-3 W	0.1-0.02 s	Wickham & Worthen 1979 [98]
Nd:YAG	4-6	-	2-6 mJ	-	Epstein 1985 [99]
Nd:YAG	4	20 µm	5-7 mJ	14 ns	Melamed 1985 [106]
Nd:YAG	4	-	40 mJ	-	Melamed 1987 [102]
Nd:YAG	10	-	10 mJ	-	Del Priore 1988 [100]
Nd:YAG	65	-	1-2.5 mJ	-	Fukuchi 1993 [101]
Excimer	3-5	0.31 µm	35-55 mJ	3 s	Vogel 1997 [103]
Excimer	10	500 µm	1.2 mJ	60 ns	Töteberg-Harms 2011 [104]

Table 2 shows the number of spots and laser settings of previous studies. The table highlights the inconsistent settings used for trabeculopuncture.

Despite all efforts, the IOP lowering effect of TP only lasted temporarily. Newly formed membranes, tissue repair, and scarring are the three main factors that lead to the failure of TP. The subsequent inflammatory response will lead to scarring or stimulate corneal endothelial cells to migrate and form a membrane over the TM, which will cover the puncture. Additionally, blood reflux into the anterior chamber brings along fibrocytes that induce fibrosis. [106] To prevent fibrosis post-interventional injections of 5-fluorouracil have been applied subconjunctivally, however without success. Attempts to reduce blood reflux have also not been the answer to the problem. [106] An invasive form of trabeculopuncture, endoscopic laser trabeculotomy with the excimer laser, is more successful in lowering IOP in glaucoma [103,104,107,108]. This approach,

however, is an invasive glaucoma surgery itself and cannot be used to test for distal outflow resistance before AIT in a meaningful way.

Today, Nd:YAG laser is widely used in ophthalmology and with high frequency, for instance for a capsulotomy, routinely performed years after cataract surgery[109], peripheral iridotomy for angle closure [110], and Descemet-puncture in ineffective non-penetrating deep sclerectomy also referred to as goniopuncture [111]. Goniopuncture after sclerectomy is performed to bypass TM with poor permeability, thereby converting it into a penetrating deep sclerectomy and should not be mistaken for trabeculopuncture [112,113]. Summarizing the previous findings, an IOP reduction ranging from about 5-16 mmHg was achieved by TP, lasting mostly for up to 1 month (Table 1). Even though TP has not yielded lasting success in glaucoma treatment, its temporary impact on the IOP might help to assess the distal outflow tract patency in humans.

Porcine eyes

Porcine eyes act as an excellent model for ophthalmic research. Despite minor differences, they share many similarities with human eyes and are therefore commonly used for ex vivo studies [80,114,115]. The size and shape of both eyeballs are alike [116]. For human corneas, a diameter of approximately 11.5 mm [117] and central thickness of about 540 µm [118] are considered normal. The cornea of domestic pigs is slightly larger and significantly thicker than human corneas; it measures approximately 15 mm horizontally and 12.5 mm vertically and is about 1000 µm thick [119]. Figure 6 depicts an enucleated porcine eye; the temporal and nasal quadrants can easily be distinguished, as the temporal curvature is distinctly steeper. Likewise, the superior curvature is marginally steeper than the inferior one.

The anterior chamber volume is estimated to be 300 µl for both human and porcine eyes [116]. Moreover, both share comparable AH outflow tracts with a wedge-shaped TM that is located between the corneal endothelium and scleral sulcus (Figure 7). The size and architecture of TM are also similar to the human TM (Figure 2) [116]. In contrast to a single and continuous SC like in humans, porcine eyes show a constellation of many smaller channels, referred to as Schlemm's canal-like segments or angular aqueous plexus (AAP) [116,120,121]. The AAP is about 5 – 30 µm in depth and 15-150 µm in length; the human SC measures 10 – 25 µm and 200 – 400 µm in depth and length, respectively. Similar to the human aqueous outflow tract, the AAP eventually drains into the episcleral venous plexus via collector channels [116]. The

equilibrium of AH production and outflow results in a mean IOP of 15.2 ± 1.8 mmHg [122] in vivo porcine eyes; this number is close to the human IOP. Sharing all these features as well as their good availability at short postmortem times makes porcine eyes a suitable model for glaucoma research.

Figure 6 Enucleated Porcine Eye

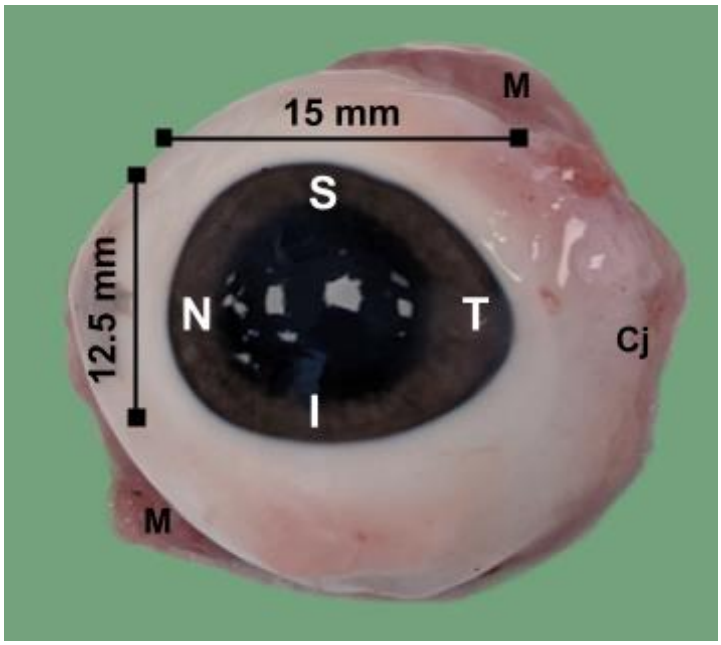

Figure 6 depicts an enucleated left porcine eye. The temporal and superior curvatures are steeper than the nasal and inferior ones, respectively. The cornea measures about 15 mm in length and 12.5 mm in height.
Cj = conjunctiva; I = inferior; M = muscle; N = nasal; S = superior; T = temporal

Figure 7 Porcine Anterior Chamber Angle

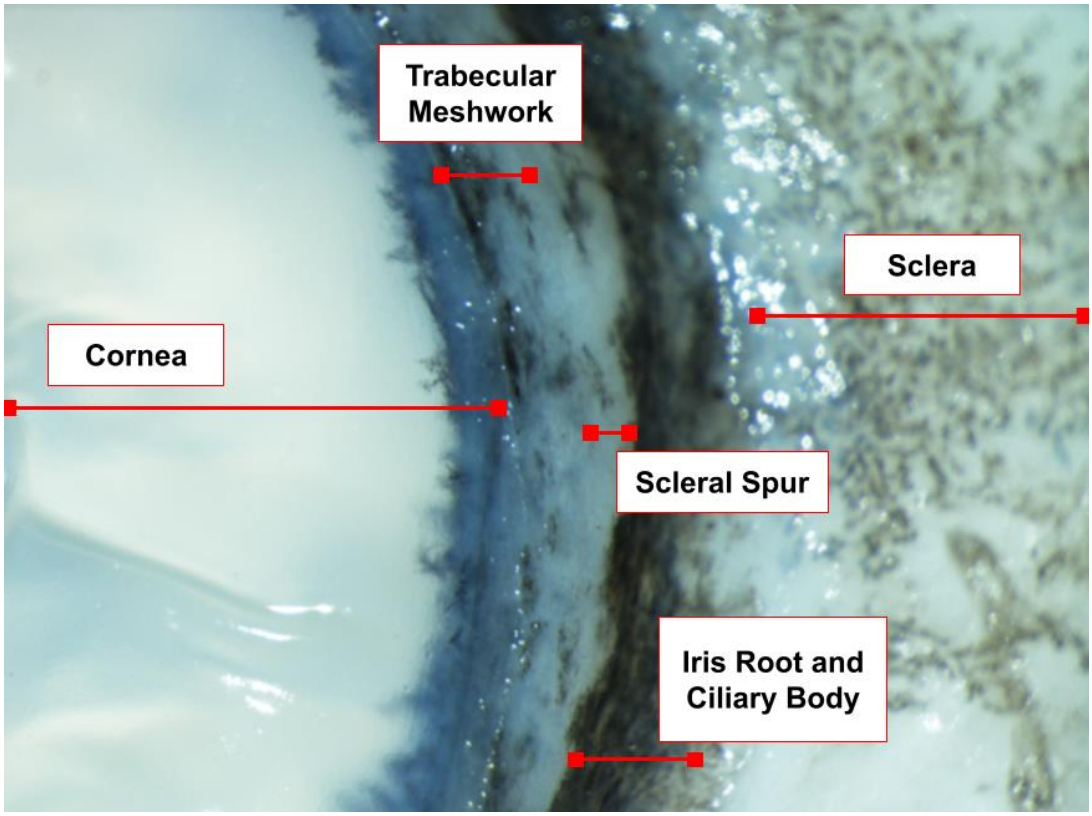

Figure 7 visualizes the porcine anterior chamber angle after blunt removal of the iris and ciliary body. Pigment deposits can be seen in the trabecular meshwork (TM) and the region of the scleral spur.

Many previous studies have used porcine eyes to investigate different surgical approaches such as AIT or trabecular micro-bypass stents [123,124]. Also, different glaucoma types can be imitated, for instance, angle-closure [125] or pigmentary glaucoma [121]. Furthermore, drug-induced changes in outflow patterns have been successfully demonstrated on porcine eyes [126,127]. For a large number of these studies, porcine anterior segments have served as research models [80,125,128]. These models consist of bisected porcine eyes that can be incubated for up to several weeks while mounted on perfusion systems [129]. For visualization of the AH outflow tract, these systems can be perfused with different fluorescent dyes or diluted microspheres to capture outflow changes [125,130]. The resulting canalograms of the outflow tract can be analyzed by fluorescence quantification or filling times [124]. Moreover, continuous ex vivo IOP measurement of anterior models is made possible with the help of pressure transducers directly connected to the perfusion system [129].

Compared to whole eyes, anterior segments can be incubated for a longer period, allowing more extensive and accurate measurements [130]. However, due to a ring that is used to fixate the bisected eye on anterior perfusion models, the episcleral might be slightly compressed and consequently elevate the EVP. Therefore, canalograms on anterior perfusion systems show less pronounced filling patterns [130]. Nevertheless, as outflow changes can still be sufficiently visualized, most studies were conducted using anterior segments on account of their many other advantages.

Hypothesis

To investigate the use of TP as a predictive test for AIT success, we conducted this pilot study deploying ex vivo porcine anterior segment models [14,15]. The use of porcine eyes allows drawing conclusions on potential outcomes in human eyes as both share main anatomical features [16,17]. Therefore, we hypothesized that a successful TP would be predictive of AIT success. We defined success for TP as 5%, and for AIT as 10% IOP reduction from baseline, respectively. These specific values were chosen as a control group of porcine anterior eyes has previously shown an IOP rise of about 5% after 40 hours and 10% after about 80 hours of incubation [129]. Hence, a 5% IOP decrease after TP truly resembles a 10% IOP reduction and a 10% decrease after AIT a 20% IOP reduction.

H0: An intraocular pressure reduction after trabeculopuncture is not predictive for the outcome of subsequent ab interno trabeculectomy.

H1: An intraocular pressure reduction after trabeculopuncture is predictive for the outcome of subsequent ab interno trabeculectomy.

2. Methods

Study design

In total, 81 hemisected porcine eyes were mounted on perfusion dishes and assigned to one of two groups: trial (T) (n = 42) and control (C) (n = 39). Eyes in the trial group underwent trabeculopuncture 24 hours after incubation using a Nd:YAG laser, followed by ab-interno trabeculectomy one day later. The IOP was measured continuously for 72 hours, with baseline values being recorded 24 hours (IOP_{BL}) after the start of the experiment. The values measured 48 and 72 hours after incubation were considered to be the post trabeculopuncture (IOP_{TP}) and the post trabeculectomy (IOP_{AIT}) values, respectively.

Eyes in the control group did not undergo any procedures; however, they were likewise incubated and had their IOPs monitored for 72 hours. IOP values were noted down at 24 hours (IOP_{BL}), 48 hours (IOP_{48}), and 72 hours (IOP_{72}) after incubation.

Perfusion dishes

Custom-made perfusion dishes were deployed to mount and to perfuse porcine eyes. They consisted of acrylic glass. Figure 8 shows the shape and dimensions of the dishes, which consist of an acrylic outer rim and ground part. Two metal tubes are connected to 0.8 mm pipes in the base that function as inflow and outflow. Bisected anterior segments were fixed in the center using a compression ring, four metal screws, and nuts (Figure 9). To facilitate handling during incubation, we designed custom-made perfusion slides and lids (Figure 10) and 3D-printed them from polylactic acid using a fused deposition modeling 3D printer (Prusa MK3S, Prusa Research a.s., Prague, Czech).

Figure 8 Perfusion Dish

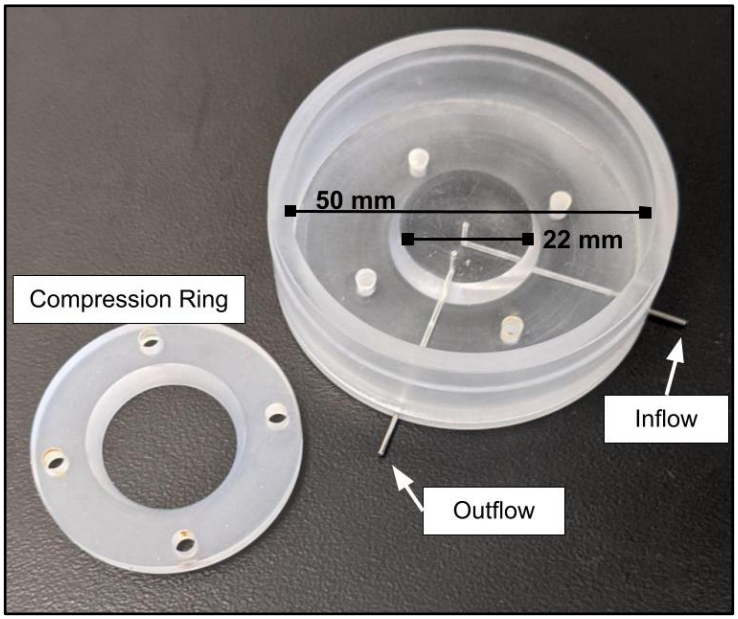

Figure 8 shows the custom-made perfusion dish and compression ring made from acrylic glass. Small pipes of 0.8 mm diameter function as in- and outflow for the perfusate.

Figure 9 Mounted and Fixated Anterior Segment

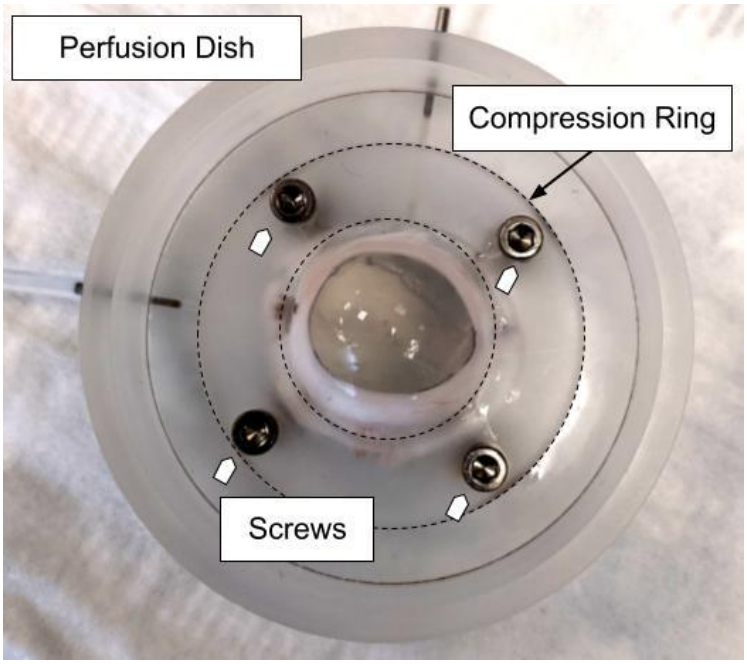

Figure 9 depicts a mounted anterior segment on a perfusion dish. Four metal screws are used to fixate the compression ring (dotted lines).

Figure 10 Mounted Anterior Segment and Perfusion Slide

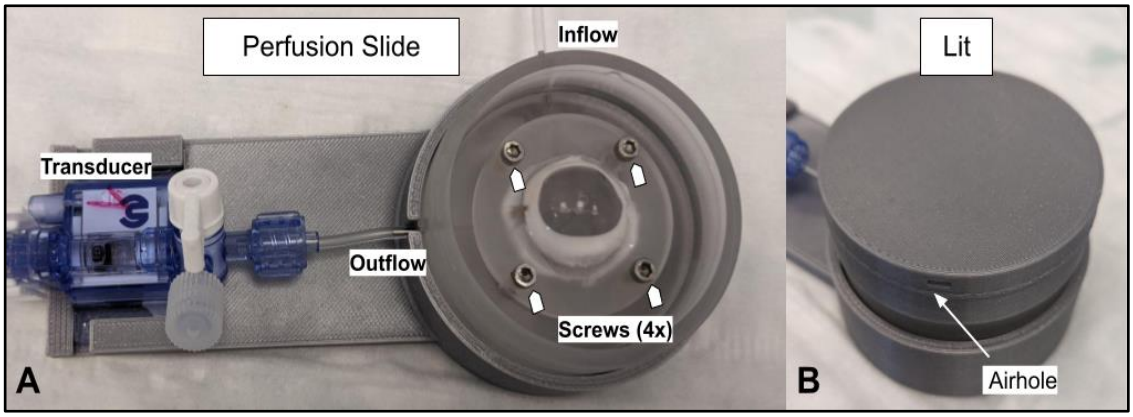

Figure 9 depicts the functional unit of the pressure transducer and the mounted anterior segment in the perfusion dish, which are both placed in the perfusion slide (A). To prevent contamination, custom-made lit with an airhole was used during incubation (B).

Laminar Flow Hood

Laminar flow hoods are ventilated devices that are used to create an aseptic work environment. A laminar flow is directed towards the user, which prevents the intrusion of pathogens into the work area. For this study, a laminar flow hood (MSC-Advantage, Thermo Fisher Scientific, Waltham, United States) was used for the aseptic preparation of porcine eyes and mounting them on anterior segments.

Incubator

An incubator is a device that is used to maintain the desired temperature, O_2-/CO_2 level, and humidity to culture cells or other organic material. As the environment in an incubator is almost germ-free, cultures can be bred over a long period with a low risk of contamination. For this study, a CO_2-incubator (HeraCell 240, Thermo Scientific Corp., Waltham, Massachusetts, United States) was used to create an atmosphere of 37.0 °C and 5.0% CO_2 level to cultivate the anterior segments. This setting has been shown to resemble the optimal atmosphere for porcine tissue.

Perfusion Pump and Perfusate

Establishing a constant inflow into mounted anterior segments was important in this study to gain stable IOP levels. A mechanically driven syringe pump (Harvard PHD ULTRA™ CP Syringe Pump, Harvard Apparatus, Holliston, Massachusetts, United States) aided in constantly perfusing the anterior segment. This pump was equipped with eight 50 ml syringes (BD Medical device company, New Jersey, United States)

filled with 30 ml DMEM to generate a constant inflow into each anterior segment simultaneously. The flow rate was set to 6 µL/min; the force level to 100%. The use of 30 mL syringes allowed constant perfusion over > 80 hours.

A cell culture medium was used for perfusion. Cell culture media provide amino acids, ions, and glucose to maintain or grow cells. Dulbecco's Modified Eagle Medium (DMEM) fortified with Penicillin and streptomycin was used as a perfusate for this experiment. This medium has been shown to be the ideal solution for TM cultures [131].

Signal Processing

Pressure transducers are commonly used for continuous, invasive blood pressure measurement. Physical deformation by air or liquid of an installed silicon diaphragm in the transducer affects connected strain gauges that lead to a change in resistance. By this, the physical signal is converted into an analog signal that is transmitted to a central processing unit. In this research work, the IOP of anterior segments was measured by deploying disposable pressure transducers equipped with a Utah connector (Daltren DPT-200, Utah Medical Products Inc., Midvale, United States). An adapter cable was used to connect each transducer to an amplifier bridge (Octal Bridge Amp, ADInstruments, Sydney, Australia) combined with a data acquisition device (PowerLab 8/35, ADInstruments, Sydney, Australia). Before every run, the transducers were calibrated using a handheld calibration device (Veri-Cal Pressure Transducer Tester, Utah Medical Products, Inc., Midvale, UT, United States). Data was processed and IOP in mmHg was continuously recorded as pressure curves over 72 hours by a physiological data analysis software (LabChart, Version 8.1.16, ADInstruments, Sydney, Australia).

Microspheres and Microscope

Microspheres are small spherical polystyrene beads incorporated with a fluorescent dye that can be visualized when irradiated with light of a certain wavelength. They provide a wide range of applications such as cell imaging, investigation of fluid dynamics, or tracking of flow ways. Using the correct concentration of spheres is essential for adequate imaging, as the fluorescent intensity can be impaired by a condition called quenching [132]. To prevent quenching, microspheres can be diluted to a lower concentration.

For this experiment 0.5 µm, the Olympus yellow-green fluorescent microspheres (FluoSpheres 0.5 µm, Thermo Fisher Scientific Inc., Waltham, Massachusetts, United States) diluted to 1:25 were deployed for outflow imaging of porcine anterior segments eyes. Phosphate-buffered saline (PBS) was used to dilute the spheres; the ratio of 1:25 (spheres:PBS) was determined by many trial runs.

A stereomicroscope (Olympus SZX, Olympus K.K., Tokyo, Japan) equipped with a 0.5x objective lens, a camera, and LED illuminator (CoolLED pE-300, CoolLED Limited, London, UK) was deployed for the visualization and capturing of fluorescent images. To induce fluorescence of the yellow-green spheres, a wavelength of 510 nm was set. For image analysis, an image processing software (Olympus cellSens Dimension, Olympus K.K., Tokyo, Japan) was used.

Preparation and Incubation

Freshly enucleated porcine eyes were obtained from a local abattoir (Landschlachterei Issing, Retzbach, Bavaria, Germany). Eyes were enucleated during evisceration by a professional abattoir. The eyes were picked up by Raoul Verma-Führing in the early morning hours, placed on ice, and processed within three hours postmortem. No animals were sacrificed purely to perform this research. All eyes were stripped of extraocular tissue using blunt forceps and ophthalmic scissors (Figure 11); then moved into a laminar flow hood. They were then placed in a 2.5% povidone-iodine solution for 30 seconds and rinsed with PBS. After bisecting them at the equator, the vitreous body, lens, and uvea were removed in one piece (Figure 12). The eviscerated eyes were subsequently mounted on our custom-made perfusion dishes and incubated at 37 °C. A constant inflow of DMEM fortified with Penicillin/Streptomycin was provided at 6 µl/min using the perfusion pump. Additionally, the eyes were connected to the pressure transducers for continuous IOP measurement; recorded with LabChart. An overview of the whole incubation process is depicted in Figure 14.

Figure 11 Removal of Extraocular Tissue

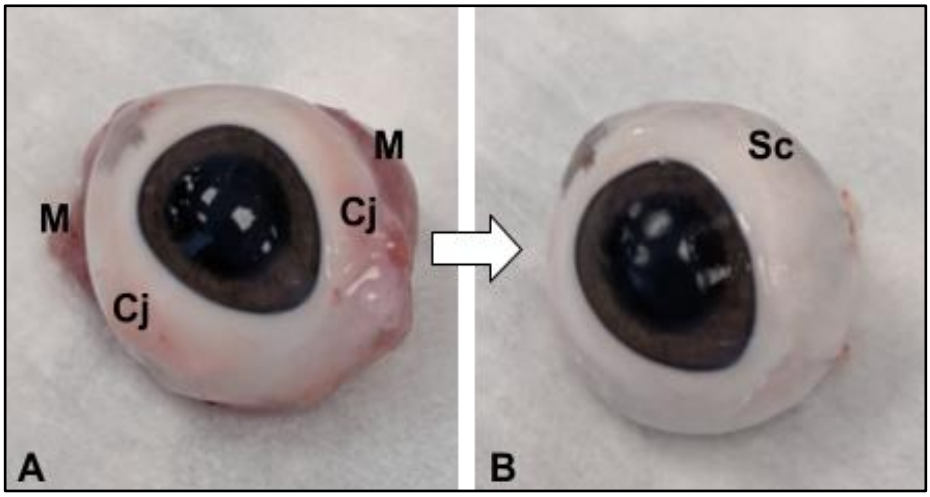

Figure 11 shows the enucleated porcine eye before (A) and after (B) removal of extraocular tissue (mostly muscles and conjunctiva). Ophthalmic scissors and blunt forceps were used for this step. The trimmed eyes were then moved to the laminar flow hood for further processing. Cj = conjunctiva; M = muscle; Sc = sclera

Figure 12 Bisection and Removal of Intraocular Tissue

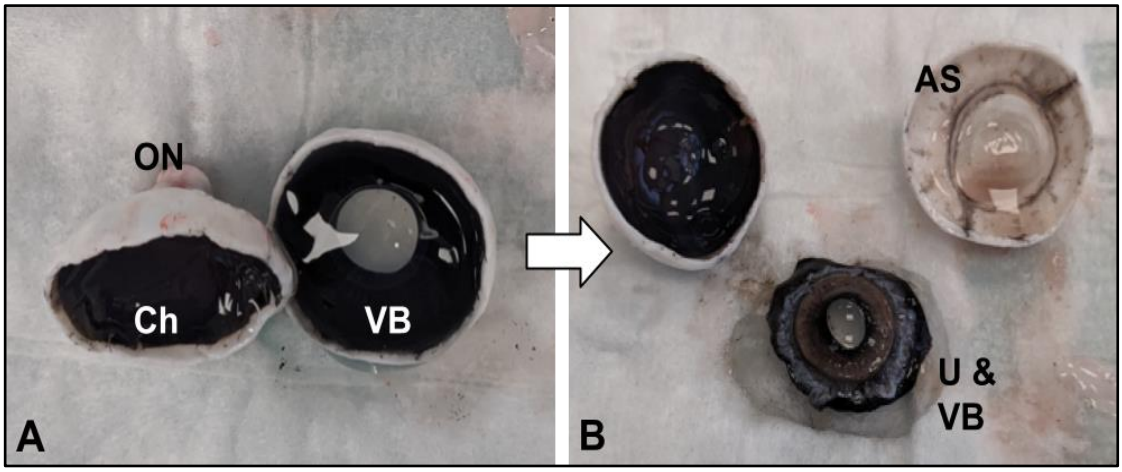

Figure 12 demonstrates the bisection at the equator (A) and subsequent removal of vitreous body and uvea (B). The remaining anterior segment was again rinsed with PBS and then mounted onto the perfusion dish. Both steps were performed under the laminar flow hood. AS = anterior segment; Ch = choroidea; ON = optic nerve; U = uvea; VB = vitreous body

Canalograms

Canalogram images at baseline, post TP, and post AIT were acquired. The outflow of the perfusion dish was temporarily left open until the anterior chamber collapsed. Eyes were then placed under the Olympus stereomicroscope and baseline canalograms were obtained using a gravity-driven infusion of diluted fluorescent microspheres. Therefore, spheres hardly pass through an intact TM. Images were recorded every 10 seconds for 10 minutes using cellSens Dimension (Version 2.3, Olympus K.K., Tokyo, Japan). Subsequently, the transmission of fluorescent spheres into the episcleral veins was visually assessed.

Trabeculopuncture and Ab Interno Trabeculectomy

After 24 hours of incubation, the anterior segments were unmounted and four evenly spread trabeculopunctures were carried out 180° along the nasal trabecular meshwork using a Q-switched Nd:YAG laser (VISULAS YAGIII, Zeiss, Oberkochen, Germany). Radiation of 7-10 mJ per shot was delivered 15 times (total energy: 100-150 mJ) for each puncture.

A 180-degree ab-interno trabeculectomy was performed 24 hours later on the same region of the TM using a Kahook Dual Blade (New World Medical, Rancho Cucamonga, California, United States).

Histology

Sagittal specimen sections were obtained from the corneal rim before TP, post-TP, and post-AIT. These were then fixed with 4% paraformaldehyde in PBS for 24 hours. After rinsing them three times in PBS, they were embedded in paraffin, sectioned at 6-micron thickness, and stained with hematoxylin and eosin.

Statistical Analysis

A sample size calculation was conducted using G*Power (Version 3.1.9.7., Heinrich Heine University, Düsseldorf, Germany). As this was a pilot study, no previous data was available. Therefore, values for the calculation were only estimated using prior results (Table 1). We assumed approximately 15-20% IOP reduction and a standard deviation of 5 mmHg. Deploying these estimates led to an effect size of about 0.5. The sample size calculation resulted in a minimum requirement of 35 eyes per group to achieve a study power of 0.9.

Acquired data was analyzed using SPSS Statistics (Version 26, IBM, New York, United States). Means and standard deviations were reported as continuous variables for IOP parameters; TP and AIT success as dichotomous variables (responders/non-responders). IOP parameters in the experimental group were defined for baseline IOP (IOP_{BL}), IOP post TP (IOP_{TP}), and IOP post AIT (IOP_{AIT}). For the control group, baseline IOP (IOP_{BL}), IOP after 48 hours (IOP_{48}), and IOP after 72 hours (IOP_{72}) were recorded. Additionally, the difference from baseline IOP after TP ($Diff_{TP}$) and AIT ($Diff_{AIT}$) in the trial, as well as after 48 hours ($Diff_{48}$) and 72 ($Diff_{72}$) hours in the control group.

TP and AIT success was defined as a decrease of 5% and 10% from baseline IOP, respectively. The Kolmogorov-Smirnov test was run to test for the normal distribution of data. A paired t-test or a Wilcoxon Signed Rank test was used to compare dependent means; an unpaired t-test or Mann-Whitney U test to compare independent means. The one-way repeated measures multivariate analysis of variances (MANOVA) was deployed to compare more than two means. As a consequence of the small sample size, Fisher's exact test was used to compare the proportion of TP responders between AIT responders and non-responders, instead of a Chi-squared test. Sensitivity, specificity, positive predictive value (PPV), and negative predictive value (NPV) were calculated for TP. A receiver operating characteristic (ROC) curve was plotted for IOP reduction after TP and AIT success. For all tests, a p-value of 0.05 or less was considered statistically significant. The statistical analysis was conducted by Raoul Verma-Führing.

Figure 13 Overview of the Whole Incubation Process

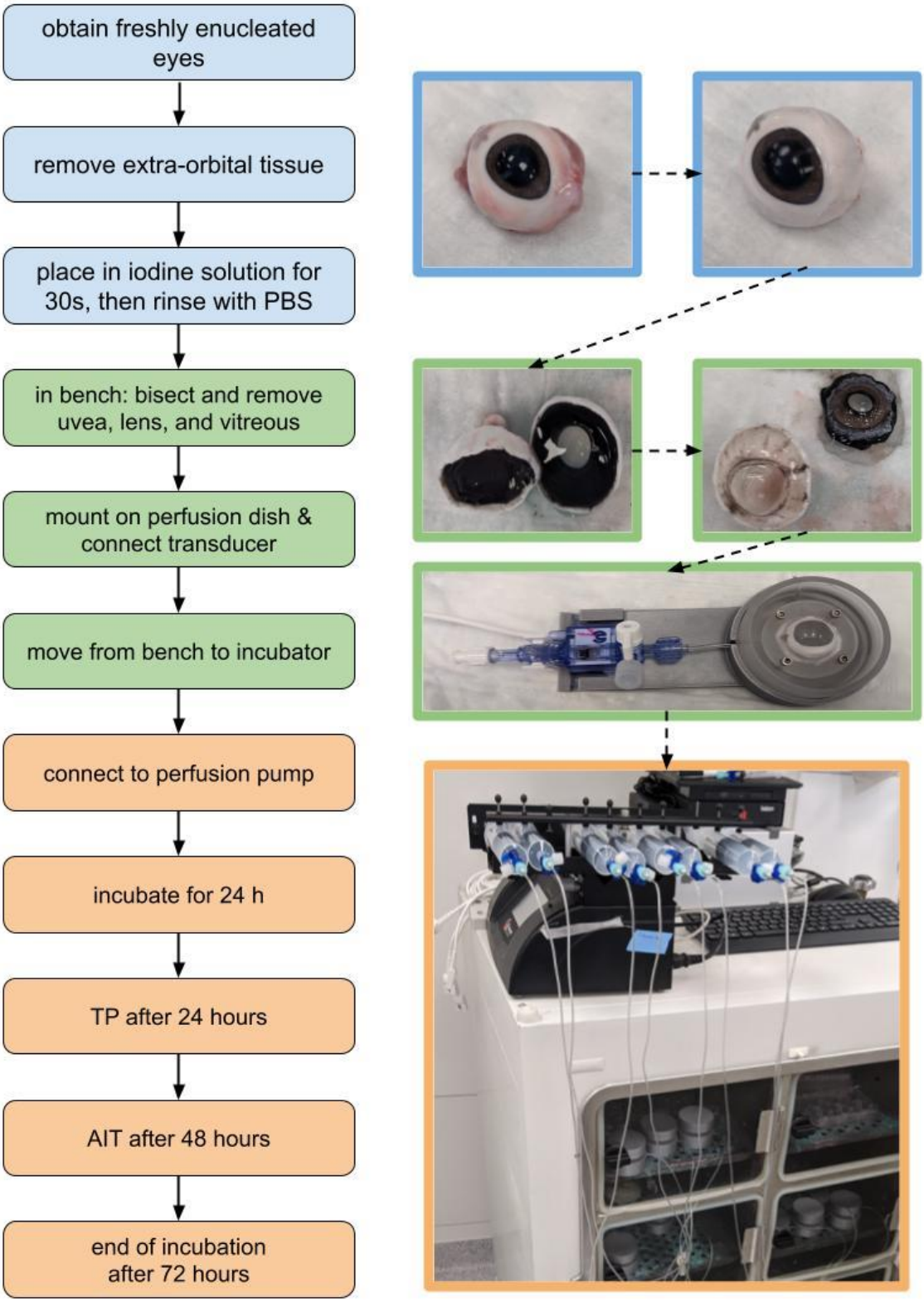

Figure 13 provides an overview of the whole incubation process.

3. Results

Pilot experiments with whole eyes showed that a transcorneal TP using a Ritch trabeculoplasty lens could not be accomplished reliably. Therefore, anterior segments were inverted and the TM to be lasered directly. The TM could be readily identified (Figure 14, BL1). The procedure resulted in small, well-circumscribed pits of approximately 500 µm in length and 250 µm in depth (Figure 14, TP1). No obvious damage to adjacent tissue was detected upon inspection with a microscope. AIT removed the TM extensively, leading to a narrow continuous groove along with the nasal quadrants (Figure 14, AIT1). The findings on histological sections (Figure 14, middle row) after both procedures corresponded well to our observations through an operating microscope. These were further supported by canalograms (Figure 14, BL3) which illustrated an improved localized outflow after TP (Figure 14, TP3) and further increased sectoral outflow in the nasal quadrants and adjacent drainage segments after AIT (Figure 14, AIT3).

A total of 81 eyes were analyzed: 42 trial eyes (T) and 39 controls (C).

An overview of the p-values for the Shapiro-Wilk normality test is provided in Table 3. All IOP values in the trial group were normally distributed; IOP_{BL} and IOP_{72} were not normally distributed in the control group. The IOP difference from baseline IOP after TP or 48 hours and after AIT or 72 hours were normally distributed in both groups except for $Diff_{AIT}$.

Table 4 depicts the IOP parameters of both groups, trial and control. The intra-group and inter-group comparisons of mean IOP values are shown in Table 5 and 6, respectively. Figure 15 additionally visualizes the intra-group IOP changes as curves. Mean baseline IOP (IOP_{BL}) was 16.4 ± 4.5 mmHg in T eyes and 15.2 ± 3.9 mmHg in C eyes. There was no statistically significant difference between both parameters ($p = 0.37$). In the experimental group, mean IOP_{TP} and IOP_{AIT} values were 14.6 ± 4.3 mm Hg and 11.3 ± 3.8 mmHg, respectively. Both values were significantly lower than IOP_{BL} ($p = 0.02$ and $p < 0.001$, for IOP_{TP} and IOP_{AIT}, respectively). The 3 IOP measurements (IOP_{BL}, $IOP_{TP,}$ and IOP_{AIT}) were also found to be significantly different from each other ($p < 0.001$). Control eyes showed a statistically significant IOP increase from baseline at 24 and 48 hours after incubation ($p > 0.05$ for both). A final increase of 2.0 ±1.3 mmHg in IOP was noted.

Table 7 depicts the proportion of TP responders in both AIT responders and AIT non-responders in the trial group. The total number of TP responders was 29 (69%); for AIT, this value was 36 (85.7%). The proportion of TP responders among AIT

responders was significantly greater than that among AIT non-responders (66.7% vs 19%, respectively, p = 0.007). The positive and negative predictive values of TP as a test for predicting AIT success were 96.6% and 38.5%, respectively. Sensitivity and specificity values were 77.7% and 83.3%, respectively (Table 8). This combination of values was portrayed in the plotted ROC curve of a 5% post-TP IOP drop predicting AIT success (Figure 15).

A subanalysis regarding AIT outcome showed a mean IOP_{BL} of 17.1 ± 4.4 mmHg and 11.9 ± 2.7 mmHg for AIT responders and AIT non-responders, respectively (Table 9); these values differed significantly (p = 0.008). There was no difference in IOP_{TP} and IOP_{AIT} in both subgroups (p = 0.484 and p = 0.448, Table 3). Out of all 13 TP non-responders, 76.9% (n = 10) showed an IOP increase after TP of at least 10%.

Canalograms illustrated an improved localized outflow after TP and further increased sectoral outflow (nasal quadrants) after AIT (Figure 14). No statistical outflow quantification was performed. Figure 17 depicts the histology section before TP, after TP, and after AIT. Prior to TP, an intact TM can be seen and SC-like segments in the deep layers. TP causes deep holes with flat coagulated margins. In contrast to TP, after AIT a deep excision can be seen with irregular margins.

Figure 14 Impact of Trabeculopuncture and Ab Interno Trabeculectomy

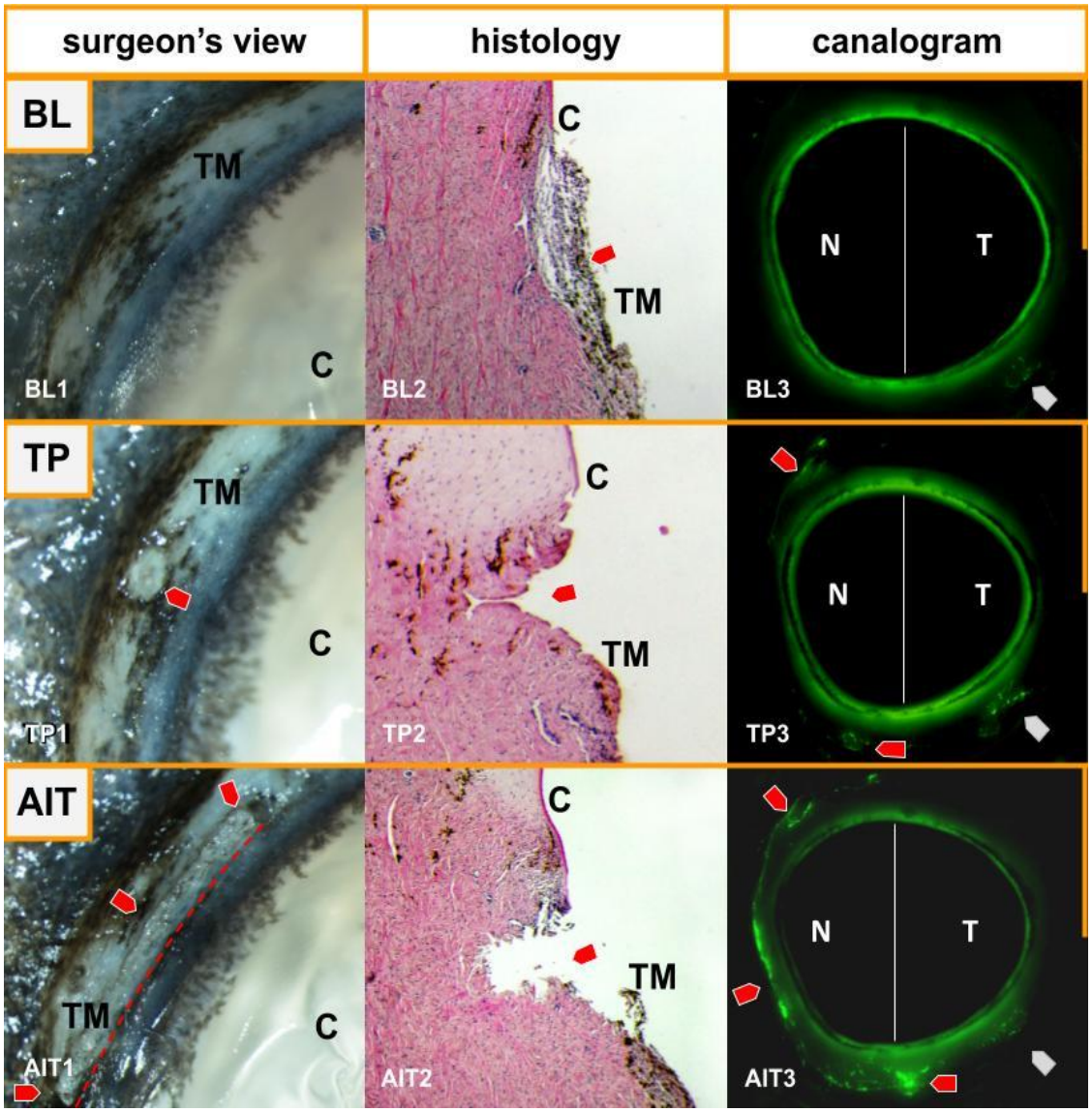

Figure 14 visualizes the effects of trabeculopuncture (TP) and ab interno trabeculectomy (AIT). Microscopic images, histology sections, and canalograms at baseline (BL), after trabeculopuncture (TP), and after ab interno trabeculectomy (AIT). **BL1:** Microscopic image of the porcine trabecular meshwork at baseline. **BL2:** Histological analysis of a section of the intact porcine TM (red arrow). **BL3:** Canalogram image of an anterior segment perfused with fluorescent spheres. No sphere collection can be in the nasal episcleral veins at baseline. Single beads were detected in the temporal region (gray arrow). **TP1:** Ex vivo image of a nasal YAG-TP. **TP2:** Histological analysis of a section after TP on the TM (red arrow). **TP3:** Canalogram image of an anterior segment perfused with fluorescent spheres after TP. Fluorescent spheres can now be visualized in the nasal episcleral veins (red arrows). Temporal fluorescence remained unchanged from baseline (gray arrow). **AIT1:** Image post trabeculectomy. The red arrows outline the excision in the TM. **AIT2:** Histological section after AIT. Trabecular meshwork is excised (red arrow). **AIT3:** Canalogram image of an anterior segment perfused with fluorescent spheres. An increased accumulation of spheres along the nasal circumference can be seen (red arrows). C = cornea; N = nasal; T = temporal; TM = trabecular meshwork

Table 3 Probability Distribution of Statistical Parameters

Overview of the probability distribution calculated by the Shapiro-Wilk normality test. IOP_{BL} = intraocular pressure at baseline; IOP_{TP} = IOP post trabeculopuncture; IOP_{AIT} = IOP post ab interno trabeculectomy; IOP_{48} = IOP after 48 hours; IOP_{72} = IOP after 72 hours; Diff = difference from baseline IOP; * = statistically significant; nd = normally distributed; non-nd = not normally distributed

Group	Parameter	P-Value	Interpretation
Trial (n = 42)	IOP_{BL}	0.16	nd
	IOP_{TP}	0.28	nd
	IOP_{AIT}	0.97	nd
	$Diff_{TP}$	0.57	nd
	$Diff_{AIT}$	0.02*	non-nd
Control (n = 39)	IOP_{BL}	0.01*	non-nd
	IOP_{48}	0.23	nd
	IOP_{72}	0.04*	non-nd
	$Diff_{48}$	0.25	nd
	$Diff_{72}$	0.27	nd

Table 4 Intraocular Pressure Parameters for Both Groups

Table 4 depicts the average, median, and minimum, and maximum intraocular pressure values for both groups.

* = statistically significant; Diff = difference from baseline IOP; IOP_{48} = IOP after 48 hours; IOP_{72} = IOP after 72 hours; IOP_{AIT} = IOP post ab interno trabeculectomy; IOP_{BL} = intraocular pressure at baseline; IOP_{TP} = IOP post trabeculopuncture; Min = lowest IOP; Max = highest IOP

Group	Parameter	Mean ± SD (mmHg)	Min - Max (mmHg)	Median (mmHg)
Trial (n = 42)	IOP_{BL}	16.4 ± 4.5	8.2 – 29.7	15.0
	IOP_{TP}	14.6 ± 4.3	7.2 – 24.4	11.2
	IOP_{AIT}	11.3 ± 3.8	2.5 – 21.2	16.2
	$Diff_{TP}$	1.7 ± 3.8	-8.0 – 12.3	2.0
	$Diff_{AIT}$	5.1 ± 4.4	-1.6 – 18.6	4.1
Control	IOP_{BL}	15.2 ± 3.9	8.0 – 21.9	15.1

(n = 39)	IOP_{48}	15.9 ± 4.0	8.9 – 23.9	17.1
	IOP_{72}	17.3 ± 4.6	10.7 – 25.6	14.5
	$Diff_{48}$	-0.8 ± 1.5	-4.7 – 3.7	-0.6
	$Diff_{72}$	-2.1 ± 2.2	-6.9 – 1.7	-1.8

Table 5 Intra-group comparison of Intraocular Pressure Values

Table 5 shows intraocular pressure (IOP) parameters and IOP changes. Trabeculopuncture and ab interno trabeculectomy led to an IOP decrease.

* = statistically significant; IOP_{48} = IOP after 48 hours; IOP_{72} = IOP after 72 hours; IOP_{AIT} = IOP post ab interno trabeculectomy; IOP_{BL} = intraocular pressure at baseline; IOP_{TP} = IOP post trabeculopuncture.

Group	Parameter	IOP-Value (mmHg)	Difference (mmHg)	P-Value for IOP Difference
Trial (n = 42)	IOP_{BL}	16.4 ± 4.5	-	-
	IOP_{TP}	14.6 ± 4.3	- 1.7 ± 3.8	0.015*
	IOP_{AIT}	11.3 ± 3.8	- 5.1 ± 4.4	< 0.001*
Control (n = 39)	IOP_{BL}	15.2 ± 3.9	-	-
	IOP_{48}	15.9 ± 4.0	0.8 ± 1.6	0.01*
	IOP_{72}	17.3 ± 4.6	2.0 ± 1.3	< 0.001*

Table 6 Inter-group comparison of Mean Intraocular Pressure Readings

Table 6 shows the comparison of mean IOP values between the trial and control groups.
* = statistically significant; IOP_{48} = IOP after 48 hours; IOP_{72} = IOP after 72 hours; IOP_{AIT} = IOP post ab interno trabeculectomy; IOP_{BL} = intraocular pressure at baseline; IOP_{TP} = IOP post trabeculopuncture.

Parameter	Trial (n = 42)	Control (n = 39)	P-Value
IOP_{BL}	16.4 ± 4.5	15.2 ± 3.9	0.37
IOP_{TP} / IOP_{48}	14.6 ± 4.3	15.9 ± 4.0	0.16
IOP_{AIT} / IOP_{72}	11.3 ± 3.8	17.3 ± 4.6	< 0.001*

Figure 15 Intraocular Pressure Curves for Both Groups

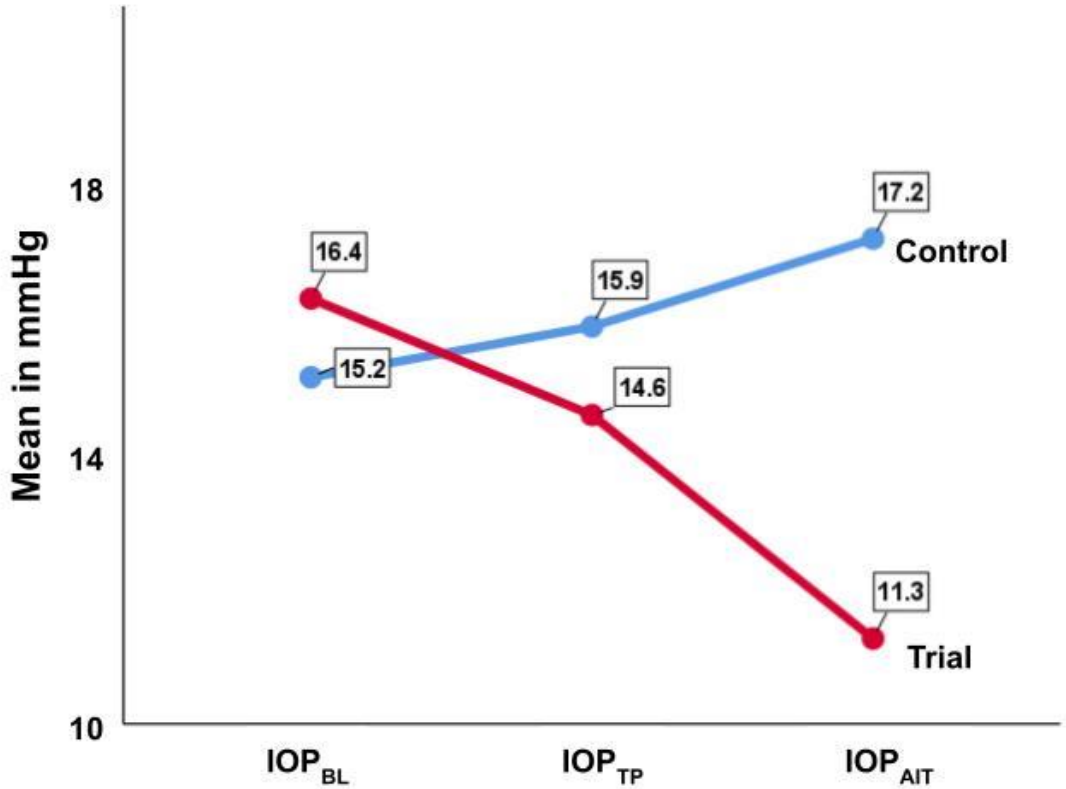

Figure 15 depicts the average intraocular pressure (IOP) readings for both groups. Trabeculopuncture and ab interno trabeculectomy resulted in an IOP decrease. The control group experienced an approximately 1 mmHg IOP increase over 72 hours of incubation. IOP_{AIT} = IOP post ab interno trabeculectomy; IOP_{BL} = intraocular pressure at baseline; IOP_{TP} = IOP post trabeculopuncture.

Table 7 Distribution Responders and Non-Responders in the Trial Group

Table 7 represents a cross table showing the proportion of TP responders in both AIT responders and AIT non-responders in the trial group.
AIT = ab interno trabeculectomy. TP = trabeculopuncture

Outcome	AIT responders (n, %)	AIT non-responders (n, %)	Total (n, %)
TP responders (n, %)	28 (66.7%)	1 (2.4%)	29 (69.0%)
TP non-responders (n, %)	8 (19.0%)	5 (11.9%)	13 (31.0%)
Total (n)	36 (85.7%)	6 (14.3%)	42 (100%)

Table 8 Sensitivity, Specificity, and Positive and Negative Predictive Values

Table 8 depicts the sensitivity and specificity in predicting the success of ab interno trabeculectomy for a 5% intraocular pressure reduction after trabeculopuncture (TP). The positive predictive value (PPV) and negative predictive value (NPV) are also shown. Even though TP has a high PPV, the NPV is rather poor.

Parameter	Value (in %)
Sensitivity	77.7
Specificity	38.3
Positive Predictive Value	96.6
Negative Predictive Value	38.5

Table 9 Subanalysis of the Trial Group

Table 9 represents a subanalysis of the trial group. Eyes are subdivided into AIT responders and non-responders. Negative values represent an increase in intraocular pressure (IOP).
AIT = ab interno trabeculectomy; IOP_{AIT} = IOP 24 hours after ab interno trabeculectomy; IOP_{BL} = baseline IOP; IOP_{TP} = IOP 24 hours after trabeculopuncture

Group	Parameter	IOP reduction (mmHg)	IOP-Value (mmHg)	p-value for IOP_{BL} reduction
AIT responders	IOP_{BL}		17.1 ± 4.4	
	IOP_{TP}	2.3	14.8 ± 4.5	0.002*
	IOP_{AIT}	6.0	11.1 ± 3.9	< 0.001*
AIT non-responders	IOP_{BL}		11.9 ± 2.7	
	IOP_{TP}	- 1.5	13.5 ± 3.4	0.53
	IOP_{AIT}	- 0.4	12.4 ± 2.6	1.0

Figure 16 Receiver Operating Characteristics Curve

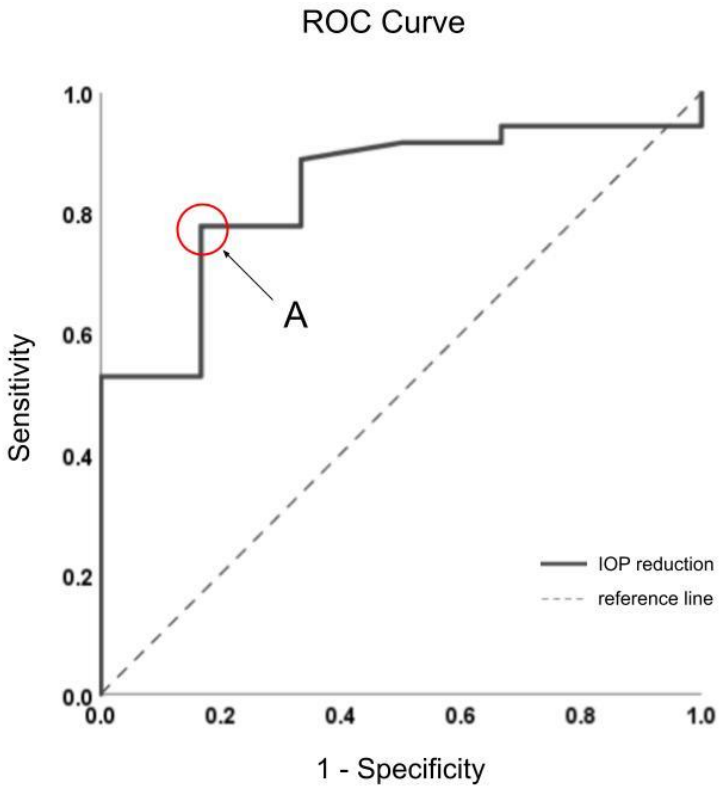

Figure 16 depicts the receiver operating characteristics (ROC) curve for post trabeculopuncture intraocular pressure (IOP) reduction in detecting ab interno trabeculectomy responders. Point A corresponds to a 5% IOP drop (resembling a 10% IOP reduction) after trabeculopuncture, representing sensitivity and specificity of 76.4% and 83.3%, respectively.

Figure 17 Histological Sections

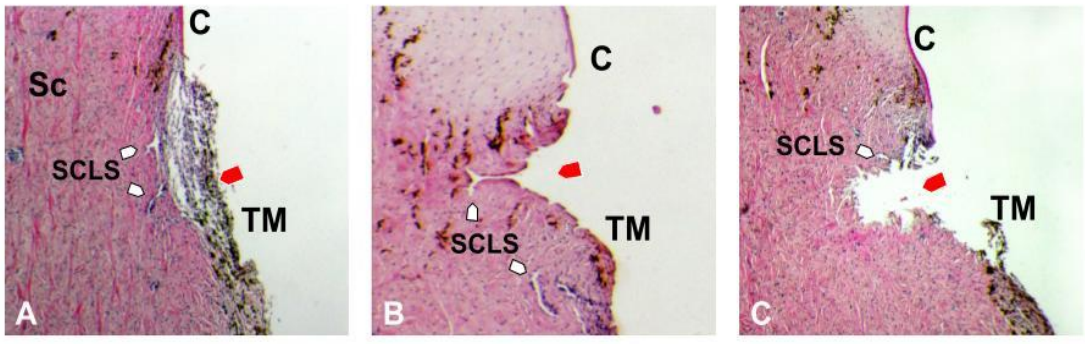

Figure 17 visualizes the histological sections before trabeculopuncture (TP) (A), after TP (B), and after ab interno trabeculectomy. The red arrows indicate the region of interest. All sections were stained with hematoxylin and eosin. The intact trabecular meshwork (TM) can be seen with Schlemm's canal-like segments in A. TP causes deep holes with flat coagulated margins (B) whereas AIT results in a deep excision with irregular margins (C).
C = cornea; Sc = sclera; SCLS = Schlemm's canal-like segments; TM = trabecular meshwork.

4. Discussion

The lack of good predictive tests combined with the relatively high rate (30%) of canal-based surgeries and implants led us to explore simple options to avoid unnecessary surgeries. Porcine eyes have been used as a model to study glaucoma extensively and were used here as well for that reason. [116,120] We used a porcine anterior segment model to assess the utility of TP in predicting the success of AIT.

We expected TP to cause an IOP drop in our porcine anterior segment perfusion model, similar to that reported in human eyes. TP is not unlike trabecular bypass stents, which also cause a focal opening in the TM, and increase outflow in a previous porcine model.[133] In human eyes, the stent placement in the TM is independent of the exact clock hour due to the continuous course of SC. Contrary to this, the angular aqueous plexus (AAP) in porcine eyes consists of several functional units that are not (or only minorly) connected to each other. Additionally, the blood reflux of in-vivo implantation indicates the right location of the micro-bypass stent; porcine anterior models lack this feedback. One TP in the porcine nasal TM circumference might not be equal to that in a human eye, and consequently would not be enough to increase the AH outflow sufficiently. On that account, we decided to perform 4 nasal TP on our porcine anterior segments (2 TP on each quarter of the nasal TM) to diminish the risk of missing a functional drainage unit. Furthermore, the amount of total energy (100-150 mJ) used was higher than what is normally required in humans due to at least three times thicker TM compared to human eyes.[116] This increased energy did not damage the surrounding tissue, as could be demonstrated microscopically and histologically. Even though the TP was performed adequately, and extensively, some eyes did not show post-interventional increased fluorescent outflow. We assumed that in these cases the AAP was missed, and no enhanced drainage could be established. However, we decided 2 TP on each quadrant to be sufficient, as the observed IOP decrease indicated an increased outflow facility.

After AIT, a further decrease in IOP was observed because of the comprehensive excision of the nasal TM using the Kahook Dual Blade. This device has previously been shown to achieve complete removal of the TM in porcine eyes [81]. The AIT was performed by only two experienced researchers over the whole course of the study to maintain the quality of the procedure. Both researchers practiced the AIT more than 20-30 porcine eyes beforehand to familiarize themselves with the handling and movement. As shown by Dang et al., this figure resembles the approximate number of eyes needed to master the procedure. [134] Fluorescent canalograms

showed surgical success by an increased outflow facility after excision of the TM, indicated by spheres entering the distal outflow tract (Figure 15).

Compared to another study by Dang et al., which tested outflow enhancement of three different AIT devices on porcine eyes, we found similar baseline IOP values (16.35 ± 4.52 mmHg vs 15.93 ± 2.08 mmHg) [135] but observed a post-AIT IOP decreased by only 31%, in contrast to 48% as reported in that study [135]. However, that research team performed the KDB-mediated AIT on only 8 eyes, which is less than a quarter of the eyes included in this study. This circumstance is most likely to account for the discrepancy in post-AIT IOP levels.

The control group in our cohort experienced a small IOP increase of approximately 13% over 72 hours. This is in line with Dang et al. who observed a 10% IOP increase in control eyes during 72 hours of incubation [129]. To adjust for this, we chose 5% and 10% to be satisfactory post-TP and post-AIT IOP reduction, respectively. These values correspond to a 10% and 20% IOP reduction after each of these procedures. Clinically, a 20% post-AIT IOP reduction is often regarded as sufficient for mild to moderate glaucoma.[87] Being able to predict this outcome will help avoid unnecessary procedures and decrease the burden on the healthcare system.

Interestingly, our subanalysis revealed that AIT responders had a higher baseline IOP compared to non-responders. This is perhaps to be expected, as AIT generally caused a greater decrease in eyes with higher baseline IOPs in clinical studies [136]. AIT non-responders also had a higher mean IOP after TP, which did not reach significance with the number examined here. It is possible that the collapse of laser-induced trabeculopunctures temporarily decreases outflow facility as described before, [94,105] which could similarly affect our non-TP responders if their TM was compromised in the area of TP and AIT. Additionally, there was no difference between baseline and post-AIT IOP levels in non-responders, which is indicative of a post-trabecular meshwork resistance in these eyes. These were not glaucomatous eyes, however. Ocular hypertension can be induced experimentally in pig eyes [121] but does not occur in pigs naturally. We suspect that inadvertent compression of key elements of the distal outflow tract in the nasal quadrants by the compression ring of the perfusion mount is responsible for this. This would not necessarily lead to an increased IOP because at least 75% of the outflow tract has to be compromised [125], but it can explain the failure to respond to TP and AIT. One has to be careful

interpreting the results of this subanalysis, however, as there were only six AIT non-responders in our study.

A simple and noninvasive predictive test for canal-based surgeries that ablate, excise, disrupt or bypass the TM is urgently needed because of the rapidly increasing demand for these procedures. The implementation of Nd:YAG laser-TP for such a test is straightforward, as this device is ubiquitously available in ophthalmology practices and clinics and most ophthalmologists are familiar with its use [137]. Although the effect of TP is too short-lived to be useful for glaucoma treatment [100,102], it is precisely this benign nature that may afford a low-risk test of distal outflow resistance.

The positive predictive value (PPV) of 96.6% for TP as a test for AIT success is promising. Moreover, our sensitivity and specificity values of 77% and 83%, respectively, are sufficient for a clinical test. Our data did not show a high negative predictive value (NPV, 38.5%) in porcine eyes, however, because these are non-glaucomatous eyes. The NPV in human eyes should be higher, matching the AIT failure rate caused by a presumed higher rate of post-trabecular resistance than in pigs.

One limitation of our study is the ex-vivo setting. Hence, wound healing of the TM and its effect on IOP cannot be observed. Another limitation is the anatomical difference between porcine eyes and human eyes. In porcine eyes, the outflow tract consists of an angular aqueous plexus, whereas humans have a Schlemm’s canal often with a single lumen. [114,138] We used four evenly spaced TPs over the nasal angle not only to cover the extent of an AIT but also because of the decreased circumferential flow compared to a human Schlemm’s canal. Clinically, reflux of blood from SC can normally be seen after a TP, a useful indicator of completion that is absent in an ex vivo model. We had to use the IOP decrease and an increased outflow of fluorescent beads as an indicator instead.

5. Conclusion

AIT is an important surgical intervention to treat mild to moderate glaucoma. However, it fails in approximately 30% of operated eyes, likely due to an unidentified post-trabecular outflow resistance. We conducted this study to investigate the applicability of TP in predicting the outcome of AIT. Since this was a pilot study, our experiments were performed ex vivo on enucleated porcine eyes, as they are easily available and share many features with human eyes. In particular, the aqueous humor outflow system is quite similar to the human outflow tract. IOP values and changes were continuously monitored and served as evaluation parameters for our statistical analysis. Although TP has been performed since the 1970s for glaucoma treatment, it has never been considered to be utilized as a potential predictive test. We found that TP has a high PPV in predicting AIT success in porcine eyes; however, the NPV was rather poor. The use of non-glaucomatous porcine eyes is likely to be the underlying reason for the low NPV as their post-trabecular outflow resistance is not increased. Human glaucoma patients probably show better results concerning the NPV and will therefore benefit from this test. In conclusion, a 10% IOP reduction after TP can be used to predict a successful AIT in porcine eyes. Whether this holds true for human individuals ought to be investigated in future clinical trials. We are confident in our results and consider the potential of TP in preventing unnecessary surgeries in glaucoma patients to be high.

Conclusion in German

Die AIT ist heutzutage ein wichtiger chirurgischer Eingriff zur Behandlung des leichten bis mittelschweren Glaukoms. Sie scheitert jedoch in etwa 30 % der operierten Fälle, was vermutlich auf einen vorher nicht identifizierten posttrabekulären Abflusswiderstand zurückzuführen ist. Wir haben diese Studie durchgeführt, um die Anwendbarkeit der TP zur Vorhersage des Ergebnisses einer AIT zu untersuchen. Da es sich um eine Pilotstudie handelte, wurden unsere Experimente ex vivo an enukleierten Schweineaugen durchgeführt. Diese sind leicht verfügbar und teilen viele Gemeinsamkeiten mit menschlichen Augen. Insbesondere das Kammerwasser-Abflusssystem ist dem menschlichen Ausflusstrakt sehr ähnlich. Die kontinuierlich erhobenen IOP-Werte und -Veränderungen dienten als Bewertungsparameter für unsere statistische Analyse. Obwohl die TP bereits seit den 1970er-Jahren zur

Glaukombehandlung durchgeführt wird, wurde sie nie als potenzieller prädiktiver Test in Betracht gezogen. Wir fanden heraus, dass die TP einen hohen PPV für die Vorhersage des AIT-Erfolgs bei Schweineaugen hat; der NPV war jedoch eher gering. Die Verwendung von nicht glaukomatösen Schweineaugen ist wahrscheinlich der Grund für diesen niedrigen NPV, da sie keinen erhöhten posttrabekulären Abflusswiderstand aufweisen. Menschliche Glaukompatienten zeigen vermutlich ein besseres Ansprechen auf diesen Test sowie besseren NPV. Zusammenfassend lässt sich sagen, dass eine 10-prozentige Senkung des Augeninnendrucks nach TP bei Schweineaugen eine erfolgreiche AIT vorhersagen kann. Ob dies auch für Menschen zutrifft, sollte in zukünftigen klinischen Studien untersucht werden. Wir sind zuversichtlich und schätzen das Potenzial der TP zur Vermeidung unnötiger Operationen bei unseren Glaukompatienten als hoch ein.

6. References

1. European Glaucoma Society. Terminology and Guidelines for Glaucoma. PubliComm;

2. Quigley HA, Broman AT. The number of people with glaucoma worldwide in 2010 and 2020. Br J Ophthalmol. 2006;90: 262–267. doi:10.1136/bjo.2005.081224

3. Allison K, Patel D, Alabi O. Epidemiology of Glaucoma: The Past, Present, and Predictions for the Future. Cureus. 2020. doi:10.7759/cureus.11686

4. Quigley HA. Number of people with glaucoma worldwide. Br J Ophthalmol. 1996;80: 389–393. doi:10.1136/bjo.80.5.389

5. Heijl A, Bengtsson B, Oskarsdottir SE. Prevalence and severity of undetected manifest glaucoma: results from the early manifest glaucoma trial screening. Ophthalmology. 2013;120: 1541–1545. doi:10.1016/j.ophtha.2013.01.043

6. Tan NYQ, Friedman DS, Stalmans I, Ahmed IIK, Sng CCA. Glaucoma screening: where are we and where do we need to go? Curr Opin Ophthalmol. 2020;31: 91–100. doi:10.1097/ICU.0000000000000649

7. Stein JD, Khawaja AP, Weizer JS. Glaucoma in Adults-Screening, Diagnosis, and Management: A Review. JAMA. 2021;325: 164–174. doi:10.1001/jama.2020.21899

8. McMonnies CW. Glaucoma history and risk factors. J Optom. 2017;10: 71–78. doi:10.1016/j.optom.2016.02.003

9. Crimmins EM. Lifespan and Healthspan: Past, Present, and Promise. Gerontologist. 2015;55: 901–911. doi:10.1093/geront/gnv130

10. Stevens W, Peneva D, Li JZ, Liu LZ, Liu G, Gao R, et al. Estimating the future burden of cardiovascular disease and the value of lipid and blood pressure control therapies in China. BMC Health Serv Res. 2016;16: 175. doi:10.1186/s12913-016-1420-8

11. Meo SA. Prevalence and future prediction of type 2 diabetes mellitus in the Kingdom of Saudi Arabia: A systematic review of published studies. J Pak Med Assoc. 2016;66: 722–725. Available: https://www.ncbi.nlm.nih.gov/pubmed/27339576

12. Vasan RS, Benjamin EJ. The Future of Cardiovascular Epidemiology. Circulation. 2016;133: 2626–2633. doi:10.1161/CIRCULATIONAHA.116.023528

13. Coleman AL, Miglior S. Risk factors for glaucoma onset and progression. Surv Ophthalmol. 2008;53 Suppl1: S3–10. doi:10.1016/j.survophthal.2008.08.006

14. Klein BE, Klein R, Linton KL. Intraocular pressure in an American community. The Beaver Dam Eye Study. Invest Ophthalmol Vis Sci. 1992;33: 2224–2228. Available: https://www.ncbi.nlm.nih.gov/pubmed/1607232

15. Goel M, Picciani RG, Lee RK, Bhattacharya SK. Aqueous humor dynamics: a review. Open Ophthalmol J. 2010;4: 52–59. doi:10.2174/1874364101004010052

16. Weinreb RN, Aung T, Medeiros FA. The pathophysiology and treatment of glaucoma: a review. JAMA. 2014;311: 1901–1911. doi:10.1001/jama.2014.3192

17. Drance SM. The early field defects in glaucoma. Invest Ophthalmol. 1969;8: 84–91. Available: https://www.ncbi.nlm.nih.gov/pubmed/5763849

18. Crawley L, Zamir SM, Cordeiro MF, Guo L. Clinical options for the reduction of elevated intraocular pressure. Ophthalmol Eye Dis. 2012;4: 43–64. doi:10.4137/OED.S4909

19. Snyder KC, Oikawa K, Williams J, Kiland JA, Gehrke S, Teixeira LBC, et al. Imaging Distal Aqueous Outflow Pathways in a Spontaneous Model of Congenital Glaucoma. Transl Vis Sci Technol. 2019;8: 22. doi:10.1167/tvst.8.5.22

20. Girkin C. Glaucoma, 2016-2017 Basic and Clinical Science Course (BCSC). American Academy of Ophthalmology; 2017.

21. Swaminathan SS, Oh D-J, Kang MH, Rhee DJ. Aqueous outflow: segmental and distal flow. J Cataract Refract Surg. 2014;40: 1263–1272. doi:10.1016/j.jcrs.2014.06.020

22. King BJ, Burns SA, Sapoznik KA, Luo T, Gast TJ. High-Resolution, Adaptive Optics Imaging of the Human Trabecular Meshwork In Vivo. Transl Vis Sci Technol. 2019;8: 5. doi:10.1167/tvst.8.5.5

23. Faralli JA, Filla MS, Peters DM. Role of Fibronectin in Primary Open Angle Glaucoma. Cells. 2019;8. doi:10.3390/cells8121518

24. Abu-Hassan DW, Acott TS, Kelley MJ. The Trabecular Meshwork: A Basic Review of Form and Function. J Ocul Biol Dis Infor. 2014;2. doi:10.13188/2334-2838.1000017

25. Carreon T, van der Merwe E, Fellman RL, Johnstone M, Bhattacharya SK. Aqueous outflow - A continuum from trabecular meshwork to episcleral veins. Prog Retin Eye Res. 2017;57: 108–133. doi:10.1016/j.preteyeres.2016.12.004

26. McDonnell F, Dismuke WM, Overby DR, Stamer WD. Pharmacological regulation of outflow resistance distal to Schlemm's canal. Am J Physiol Cell Physiol. 2018;315: C44–C51. doi:10.1152/ajpcell.00024.2018

27. Battista SA, Lu Z, Hofmann S, Freddo T, Overby DR, Gong H. Reduction of the available area for aqueous humor outflow and increase in meshwork herniations into collector channels following acute IOP elevation in bovine eyes. Invest Ophthalmol Vis Sci. 2008;49: 5346–5352. doi:10.1167/iovs.08-1707

28. Allingham RR, de Kater AW, Ethier CR. Schlemm's canal and primary open angle glaucoma: correlation between Schlemm's canal dimensions and outflow facility. Exp Eye Res. 1996;62: 101–109. doi:10.1006/exer.1996.0012

29. Usha Tejaswini S, Sivakumar P, Upadhyaya S, Venkatesh R. Elevated episcleral venous pressure and its implications: A case of Radius-Maumenee syndrome. Indian J Ophthalmol. 2020;68: 1683–1685. doi:10.4103/ijo.IJO_2407_19

30. Grieshaber MC, Pienaar A, Olivier J, Stegmann R. Clinical evaluation of the aqueous outflow system in primary open-angle glaucoma for canaloplasty. Invest Ophthalmol Vis Sci. 2010;51: 1498–1504. doi:10.1167/iovs.09-4327

31. Gong H, Francis A. Schlemm's Canal and Collector Channels as Therapeutic Targets. In: Samples JR, Ahmed IIK, editors. Surgical Innovations in Glaucoma. New York, NY: Springer New York; 2014. pp. 3–25. doi:10.1007/978-1-4614-8348-9_1

32. Tham Y-C, Li X, Wong TY, Quigley HA, Aung T, Cheng C-Y. Global prevalence of glaucoma and projections of glaucoma burden through 2040: a systematic review and meta-analysis. Ophthalmology. 2014;121: 2081–2090. doi:10.1016/j.ophtha.2014.05.013

33. Zhang N, Wang J, Chen B, Li Y, Jiang B. Prevalence of Primary Angle Closure Glaucoma in the Last 20 Years: A Meta-Analysis and Systematic Review. Front Med. 2020;7: 624179. doi:10.3389/fmed.2020.624179

34. Hall AJH. Secondary glaucoma. Clin Exp Optom. 2000;83: 190–194. doi:10.1111/j.1444-0938.2000.tb04914.x

35. Cohen LP, Pasquale LR. Clinical characteristics and current treatment of glaucoma. Cold Spring Harb Perspect Med. 2014;4. doi:10.1101/cshperspect.a017236

36. Gazzard G, Konstantakopoulou E, Garway-Heath D, Garg A, Vickerstaff V, Hunter R, et al. Selective laser trabeculoplasty versus eye drops for first-line treatment of ocular hypertension and glaucoma (LiGHT): a multicentre randomised controlled trial. Lancet. 2019;393: 1505–1516. doi:10.1016/S0140-6736(18)32213-X

37. Tanna AP. 2021-2022 BASIC AND CLINICAL SCIENCE COURSE, SECTION 10: Glaucoma. Amer Academy Of Ophthalmo; 2021. Available: https://play.google.com/store/books/details?id=VcJ6zgEACAAJ

38. Moshirfar M, Parker L, Birdsong OC, Ronquillo YC, Hofstedt D, Shah TJ, et al. Use of Rho kinase Inhibitors in Ophthalmology: A Review of the Literature. Med Hypothesis Discov Innov Ophthalmol. 2018;7: 101–111. Available: https://www.ncbi.nlm.nih.gov/pubmed/30386798

39. Zimmerman TJ. Topical ophthalmic beta blockers: a comparative review. J Ocul Pharmacol. 1993;9: 373–384. doi:10.1089/jop.1993.9.373

40. Ayala M, Chen E. Comparison of selective laser trabeculoplasty (SLT) in primary open angle glaucoma and pseudoexfoliation glaucoma. Clin Ophthalmol. 2011;5: 1469–1473. doi:10.2147/OPTH.S25636

41. Kollias N, Baqer AH. Absorption mechanisms of human melanin in the visible, 400-720 nm. J Invest Dermatol. 1987;89: 384–388. doi:10.1111/1523-1747.ep12471764

42. Damji KF, Bovell AM, Hodge WG, Rock W, Shah K, Buhrmann R, et al. Selective laser trabeculoplasty versus argon laser trabeculoplasty: results from a 1-year randomised clinical trial. Br J Ophthalmol. 2006;90: 1490–1494. doi:10.1136/bjo.2006.098855

43. Gulati V, Fan S, Gardner BJ, Havens SJ, Schaaf MT, Neely DG, et al. Mechanism of Action of Selective Laser Trabeculoplasty and Predictors of Response. Invest Ophthalmol Vis Sci. 2017;58: 1462–1468. doi:10.1167/iovs.16-20710

44. Jha B, Bhartiya S, Sharma R, Arora T, Dada T. Selective Laser Trabeculoplasty: An Overview. J Curr Glaucoma Pract. 2012;6: 79–90. doi:10.5005/jp-journals-10008-1111

45. Bartley GB, Parshley DE, Bradley JMB, Fisk A, Hadaegh A, Samples JR, et al. Laser trabeculoplasty induces stromelysin expression by trabecular juxtacanalicular cells. American Journal of Ophthalmology. 1996. p. 141. doi:10.1016/s0002-9394(14)71987-7

46. Garg A, Vickerstaff V, Nathwani N, Garway-Heath D, Konstantakopoulou E, Ambler G, et al. Efficacy of Repeat Selective Laser Trabeculoplasty in Medication-Naive Open-Angle Glaucoma and Ocular Hypertension during the LiGHT Trial. Ophthalmology. 2020;127: 467–476. doi:10.1016/j.ophtha.2019.10.023

47. Wise JB, Witter SL. Argon laser therapy for open-angle glaucoma. A pilot study. Arch Ophthalmol. 1979;97: 319–322. doi:10.1001/archopht.1979.01020010165017

48. Smith J. Argon laser trabeculoplasty: comparison of bichromatic and monochromatic wavelengths. Ophthalmology. 1984;91: 355–360. Available: https://www.ncbi.nlm.nih.gov/pubmed/6371649

49. van der Zypen E, Bebie H, Fankhauser F. Morphological studies about the efficiency of laser beams upon the structures of the angle of the anterior chamber. Facts and concepts

related to the treatment of the chronic simple glaucoma. Int Ophthalmol. 1979;1: 109–122. doi:10.1007/BF00154198

50. Jay JL, Murray SB. Early trabeculectomy versus conventional management in primary open angle glaucoma. Br J Ophthalmol. 1988;72: 881–889. doi:10.1136/bjo.72.12.881

51. Morgan WH, Yu D-Y. Surgical management of glaucoma: a review. Clin Experiment Ophthalmol. 2012;40: 388–399. doi:10.1111/j.1442-9071.2012.02769.x

52. Jampel HD, Musch DC, Gillespie BW, Lichter PR, Wright MM, Guire KE, et al. Perioperative complications of trabeculectomy in the collaborative initial glaucoma treatment study (CIGTS). Am J Ophthalmol. 2005;140: 16–22. doi:10.1016/j.ajo.2005.02.013

53. Edmunds B, Thompson JR, Salmon JF, Wormald RP. The National Survey of Trabeculectomy. III. Early and late complications. Eye . 2002;16: 297–303. doi:10.1038/sj.eye.6700148

54. Olayanju JA, Hassan MB, Hodge DO, Khanna CL. Trabeculectomy-related complications in Olmsted County, Minnesota, 1985 through 2010. JAMA Ophthalmol. 2015;133: 574–580. doi:10.1001/jamaophthalmol.2015.57

55. Gedde SJ, Schiffman JC, Feuer WJ, Herndon LW, Brandt JD, Budenz DL, et al. Three-year follow-up of the tube versus trabeculectomy study. Am J Ophthalmol. 2009;148: 670–684. doi:10.1016/j.ajo.2009.06.018

56. Batlle JF, Corona A, Albuquerque R. Long-term results of the PRESERFLO MicroShunt in patients with primary open-angle glaucoma from a single-center nonrandomized study. J Glaucoma. 2021;30: 281–286. doi:10.1097/IJG.0000000000001734

57. Buffault J, Baudouin C, Labbé A. XEN® Gel Stent for management of chronic open angle glaucoma: A review of the literature. J Fr Ophtalmol. 2019;42: e37–e46. doi:10.1016/j.jfo.2018.12.002

58. Pillunat KR, Herber R, Haase MA, Jamke M, Jasper CS, Pillunat LE. PRESERFLOTM MicroShunt versus trabeculectomy: first results on efficacy and safety. Acta Ophthalmol. 2021. doi:10.1111/aos.14968

59. Theilig T, Rehak M, Busch C, Bormann C, Schargus M, Unterlauft JD. Comparing the efficacy of trabeculectomy and XEN gel microstent implantation for the treatment of primary open-angle glaucoma: a retrospective monocentric comparative cohort study. Sci Rep. 2020;10: 19337. doi:10.1038/s41598-020-76551-y

60. Rezkallah A, Mathis T, Denis P, Kodjikian L. XEN gel stent: a total delayed-onset postoperative hyphema. Int J Ophthalmol. 2019;12: 1224–1226. doi:10.18240/ijo.2019.07.27

61. Allingham RR, Moroi S, Shields MB, Damji K. Shields' textbook of glaucoma. Lippincott Williams & Wilkins; 2020.

62. Lee RMH, Bouremel Y, Eames I, Brocchini S, Khaw PT. Translating Minimally Invasive Glaucoma Surgery Devices. Clin Transl Sci. 2020;13: 14–25. doi:10.1111/cts.12660

63. Ansari E. An Update on Implants for Minimally Invasive Glaucoma Surgery (MIGS). Ophthalmol Ther. 2017;6: 233–241. doi:10.1007/s40123-017-0098-2

64. Richter GM, Coleman AL. Minimally invasive glaucoma surgery: current status and future prospects. Clin Ophthalmol. 2016;10: 189–206. doi:10.2147/OPTH.S80490

65. Iordanous Y, Kent JS, Hutnik CML, Malvankar-Mehta MS. Projected cost comparison of Trabectome, iStent, and endoscopic cyclophotocoagulation versus glaucoma medication in the Ontario Health Insurance Plan. J Glaucoma. 2014;23: e112–8. doi:10.1097/IJG.0b013e31829d9bc7

66. Patel I, de Klerk TA, Au L. Manchester iStent study: early results from a prospective UK case series. Clin Experiment Ophthalmol. 2013;41: 648–652. doi:10.1111/ceo.12098

67. Pillunat LE, Erb C, Jünemann AG, Kimmich F. Micro-invasive glaucoma surgery (MIGS): a review of surgical procedures using stents. Clin Ophthalmol. 2017;11: 1583–1600. doi:10.2147/OPTH.S135316

68. Samuelson TW, Sarkisian SR Jr, Lubeck DM, Stiles MC, Duh Y-J, Romo EA, et al. Prospective, Randomized, Controlled Pivotal Trial of an Ab Interno Implanted Trabecular Micro-Bypass in Primary Open-Angle Glaucoma and Cataract: Two-Year Results. Ophthalmology. 2019;126: 811–821. doi:10.1016/j.ophtha.2019.03.006

69. Ziaei H, Au L. Manchester iStent study: long-term 7-year outcomes. Eye . 2021;35: 2277–2282. doi:10.1038/s41433-020-01255-6

70. Shingleton BJ, Gamell LS, O'Donoghue MW, Baylus SL, King R. Long-term changes in intraocular pressure after clear corneal phacoemulsification: normal patients versus glaucoma suspect and glaucoma patients. J Cataract Refract Surg. 1999;25: 885–890. doi:10.1016/s0886-3350(99)00107-8

71. Kim DD, Doyle JW, Smith MF. Intraocular pressure reduction following phacoemulsification cataract extraction with posterior chamber lens implantation in glaucoma patients. Ophthalmic Surg Lasers. 1999;30: 37–40. Available: https://www.ncbi.nlm.nih.gov/pubmed/9923491

72. Chen Y-Y, Lai Y-J, Yen Y-F, Huang L-Y. Use of iStent as a Standalone Operation in Patients with Open-Angle Glaucoma. J Ophthalmol. 2020;2020: 8754730. doi:10.1155/2020/8754730

73. Le K, Saheb H. iStent trabecular micro-bypass stent for open-angle glaucoma. Clin Ophthalmol. 2014;8: 1937–1945. doi:10.2147/OPTH.S45920

74. Minckler D, Baerveldt G, Ramirez MA, Mosaed S, Wilson R, Shaarawy T, et al. Clinical results with the Trabectome, a novel surgical device for treatment of open-angle glaucoma. Trans Am Ophthalmol Soc. 2006;104: 40–50. Available: https://www.ncbi.nlm.nih.gov/pubmed/17471324

75. Barkan O. GONIOTOMY FOR THE RELIEF OF CONGENITAL GLAUCOMA. Br J Ophthalmol. 1948;32: 701–728. doi:10.1136/bjo.32.9.701

76. ElMallah MK, Seibold LK, Kahook MY, Williamson BK, Singh IP, Dorairaj SK, et al. 12-Month Retrospective Comparison of Kahook Dual Blade Excisional Goniotomy with Istent Trabecular Bypass Device Implantation in Glaucomatous Eyes at the Time of Cataract Surgery. Adv Ther. 2019;36: 2515–2527. doi:10.1007/s12325-019-01025-1

77. Ramjiani V, Mudhar H-S, Julian T, Auger G. Sampling trabecular meshwork using TrabEx. BMC Ophthalmol. 2021;21: 138. doi:10.1186/s12886-021-01895-6

78. Parikh HA BSc, Roy P MD, Dhaliwal A BSc, Kaplowitz KB MD, Loewen NA MD. Trabectome patient selection, preparation, technique, management, and outcomes. US Ophthalmic Rev. 2015;08: 103. doi:10.17925/usor.2015.08.02.103

79. Kaplowitz K, Schuman JS, Loewen NA. Techniques and outcomes of minimally invasive trabecular ablation and bypass surgery. Br J Ophthalmol. 2014;98: 579–585.

doi:10.1136/bjophthalmol-2013-304256

80. Wang C, Dang Y, Waxman S, Xia X, Weinreb RN, Loewen NA. Angle stability and outflow in dual blade ab interno trabeculectomy with active versus passive chamber management. PLoS One. 2017;12: e0177238. doi:10.1371/journal.pone.0177238

81. Ammar DA, Seibold L, Kahook MY. Preclinical investigation of ab interno goniotomy using four different techniques. Invest Ophthalmol Vis Sci. 2020;61: 955–955. Available: https://iovs.arvojournals.org/article.aspx?articleid=2766810

82. Bendel RE, Patterson MT. Long-term Effectiveness of Trabectome (Ab-interno Trabeculectomy) Surgery. J Curr Glaucoma Pract. 2018;12: 119–124. doi:10.5005/jp-journals-10028-1256

83. Habash AA, Al Habash A, Al Buainain A. Long Term Outcome of Combined Phacoemulsification and Excisional Goniotomy with the Kahook Dual Blade in Different Subtypes of Glaucoma. doi:10.21203/rs.3.rs-114530/v1

84. Al Yousef Y, Strzalkowska A, Hillenkamp J, Rosentreter A, Loewen NA. Comparison of a second-generation trabecular bypass (iStent inject) to ab interno trabeculectomy (Trabectome) by exact matching. Graefes Arch Clin Exp Ophthalmol. 2020. doi:10.1007/s00417-020-04933-z

85. Okeke CO, Miller-Ellis E, Rojas M, Trabectome Study Group. Trabectome success factors. Medicine . 2017;96: e7061. doi:10.1097/MD.0000000000007061

86. Kaplowitz K, Bussel II, Honkanen R, Schuman JS, Loewen NA. Review and meta-analysis of ab-interno trabeculectomy outcomes. Br J Ophthalmol. 2016;100: 594–600. doi:10.1136/bjophthalmol-2015-307131

87. Ahuja Y, Ma Khin Pyi S, Malihi M, Hodge DO, Sit AJ. Clinical results of ab interno trabeculotomy using the trabectome for open-angle glaucoma: the Mayo Clinic series in Rochester, Minnesota. Am J Ophthalmol. 2013;156: 927–935.e2. doi:10.1016/j.ajo.2013.06.001

88. Gedde S, Vinod K. Ab interno trabeculectomy: patient selection and perspectives. Clinical Ophthalmology. 2016. pp. 1557–1564. doi:10.2147/opth.s99746

89. Traverso CE, Walt JG, Kelly SP, Hommer AH, Bron AM, Denis P, et al. Direct costs of glaucoma and severity of the disease: a multinational long term study of resource utilisation in Europe. Br J Ophthalmol. 2005;89: 1245–1249. doi:10.1136/bjo.2005.067355

90. Höhn R, Nickels S, Schuster AK, Wild PS, Münzel T, Lackner KJ, et al. Prevalence of glaucoma in Germany: results from the Gutenberg Health Study. Graefes Arch Clin Exp Ophthalmol. 2018;256: 1695–1702. doi:10.1007/s00417-018-4011-z

91. Wenzel M, Burkhard Dick H, Scharrer A, Schayan K, Agostini H, Reinhard T. Ambulante und stationäre Intraokularchirurgie 2019: Ergebnisse der aktuellen Umfrage von BDOC, BVA, DGII und DOG.

92. Krasnov MM. Laseropuncture of anterior chamber angle in glaucoma. Am J Ophthalmol. 1973;75: 674–678. doi:10.1016/0002-9394(73)90819-2

93. Krasnov MM. [Laser puncture of the anterior chamber angle in glaucoma (a preliminary report)]. Vestn Oftalmol. 1972;3: 27–31. Available: https://www.ncbi.nlm.nih.gov/pubmed/5078295

94. Rassow B, Witschel B. [Laser-trabecular puncture. Experimental studies]. Ophthalmologica. 1975;170: 362–369. doi:10.1159/000307234

95. Wickham MG, Worthen DM, Binder PS. Physiological effects of laser trabeculotomy in rhesus monkey eyes. Invest Ophthalmol Vis Sci. 1977;16: 624–628. Available: https://www.ncbi.nlm.nih.gov/pubmed/406214

96. Worthen DM, Wickham MG. Laser trabeculotomy in monkeys. Invest Ophthalmol. 1973;12: 707–711. Available: https://www.ncbi.nlm.nih.gov/pubmed/4200445

97. Worthen DM, Wickham MG. Argon laser trabeculotomy. Trans Am Acad Ophthalmol Otolaryngol. 1974;78: OP371–5. Available: https://www.ncbi.nlm.nih.gov/pubmed/4856873

98. Wickham MG, Worthen DM. Argon laser trabeculotomy:long-term follow-up. Ophthalmology. 1979;86: 495–503. doi:10.1016/s0161-6420(79)35492-6

99. Epstein DL, Melamed S, Puliafto CA, Steinert RF. Neodymium: YAG laser trabeculopuncture in open-angle glaucoma. Ophthalmology. 1985;92: 931–937. doi:10.1016/s0161-6420(85)33932-5

100. Del Priore LV, Robin AL, Pollack IP. Long-term follow-up of neodymium: YAG laser angle surgery for open-angle glaucoma. Ophthalmology. 1988;95: 277–281. doi:10.1016/s0161-6420(88)33195-7

101. Fukuchi T, Iwata K, Sawaguchi S, Nakayama T, Watanabe J. Nd:YAG laser trabeculopuncture (YLT) for glaucoma with traumatic angle recession. Graefes Arch Clin Exp Ophthalmol. 1993;231: 571–576. doi:10.1007/BF00936520

102. Melamed S, Latina MA, Epstein DL. Neodymium:YAG laser trabeculopuncture in juvenile open-angle glaucoma. Ophthalmology. 1987;94: 163–170. doi:10.1016/s0161-6420(87)33481-5

103. Vogel M, Lauritzen K. Punktuelle Excimerlaserablation des Trabekelwerks Klinische Ergebnisse. Ophthalmologe. 1997;94: 665–667. Available: https://idp.springer.com/authorize/casa?redirect_uri=https://link.springer.com/article/10.1007/s003470050180&casa_token=G5Y-fZs94OIAAAAA:9CGhWxiKFC6ZK8Dh04aWtzmLu0QgCmgRIzoGLbHZceBmSnxkizuJX_pb98N3dSOeQxIbrRpCYn0GypLq

104. Töteberg-Harms M, Ciechanowski PP, Hirn C, Funk J. [One-year results after combined cataract surgery and excimer laser trabeculotomy for elevated intraocular pressure]. Ophthalmologe. 2011;108: 733–738. doi:10.1007/s00347-011-2337-6

105. Ticho U, Cadet JC, Mahler J, Sekeles E, Bruchim A. Argon laser trabeculotomies in primates: evaluation by histological and perfusion studies. Invest Ophthalmol Vis Sci. 1978;17: 667–674. Available: https://www.ncbi.nlm.nih.gov/pubmed/97242

106. Melamed S, Pei J, Puliafito CA, Epstein DL. Q-switched neodymium-YAG laser trabeculopuncture in monkeys. Arch Ophthalmol. 1985;103: 129–133. Available: https://jamanetwork.com/journals/jamaophthalmology/article-abstract/635378

107. Durr GM, Töteberg-Harms M, Lewis R, Fea A, Marolo P, Ahmed IIK. Current review of Excimer laser Trabeculostomy. Eye Vis (Lond). 2020;7: 24. doi:10.1186/s40662-020-00190-7

108. Töteberg-Harms M, Hanson JVM, Funk J. Cataract Surgery combined with excimer laser trabeculotomy to lower intraocular pressure: effectiveness dependent on preoperative IOP. BMC Ophthalmology. 2013. doi:10.1186/1471-2415-13-24

109. Leysen I, Coeckelbergh T, Gobin L, Smet H, Daniel Y, De Groot V, et al. Cumulative neodymium:YAG laser rates after bag-in-the-lens and lens-in-the-bag intraocular lens implantation. Journal of Cataract and Refractive Surgery. 2006. pp. 2085–2090.

doi:10.1016/j.jcrs.2006.07.025

110. Huang G, Gonzalez E, Lee R, Osmonavic S, Leeungurasatien T, He M, et al. Anatomic Predictors for Anterior Chamber Angle Opening After Laser Peripheral Iridotomy in Narrow Angle Eyes. Current Eye Research. 2012. pp. 575–582. doi:10.3109/02713683.2012.655396

111. Alp MN, Yarangumeli A, Koz OG, Kural G. Nd:YAG laser goniopuncture in viscocanalostomy: penetration in non-penetrating glaucoma surgery. Int Ophthalmol. 2010;30: 245–252. doi:10.1007/s10792-009-9312-0

112. Tam DY, Barnebey HS, Ahmed IIK. Nd: YAG laser goniopuncture: indications and procedure. J Glaucoma. 2013;22: 620–625. doi:10.1097/IJG.0b013e31824d512a

113. Al Obeidan SA. Incidence, efficacy and safety of YAG laser goniopuncture following nonpenetrating deep sclerectomy at a university hospital in Riyadh, Saudi Arabia. Saudi J Ophthalmol. 2015;29: 95–102. doi:10.1016/j.sjopt.2014.09.015

114. Lei Y, Overby DR, Read AT, Stamer WD, Ethier CR. A new method for selection of angular aqueous plexus cells from porcine eyes: a model for Schlemm's canal endothelium. Invest Ophthalmol Vis Sci. 2010;51: 5744–5750. doi:10.1167/iovs.10-5703

115. Loewen RT, Roy P, Park DB, Jensen A, Scott G, Cohen-Karni D, et al. A Porcine Anterior Segment Perfusion and Transduction Model With Direct Visualization of the Trabecular Meshwork. Invest Ophthalmol Vis Sci. 2016;57: 1338–1344. doi:10.1167/iovs.15-18125

116. McMenamin PG, Steptoe RJ. Normal anatomy of the aqueous humour outflow system in the domestic pig eye. J Anat. 1991;178: 65–77. Available: https://www.ncbi.nlm.nih.gov/pubmed/1810936

117. Rüfer F, Schröder A, Erb C. White-to-white corneal diameter: normal values in healthy humans obtained with the Orbscan II topography system. Cornea. 2005;24: 259–261. doi:10.1097/01.ico.0000148312.01805.53

118. Wolfs RC, Klaver CC, Vingerling JR, Grobbee DE, Hofman A, de Jong PT. Distribution of central corneal thickness and its association with intraocular pressure: The Rotterdam Study. Am J Ophthalmol. 1997;123: 767–772. doi:10.1016/s0002-9394(14)71125-0

119. Faber C, Scherfig E, Prause JU, Sørensen KE. Corneal thickness in pigs measured by ultrasound pachymetry in vivo. Scandinavian Journal of Laboratory Animal Sciences. 2008;35: 39–43. Available: https://www.researchgate.net/profile/Carsten-Faber/publication/203045522_Corneal_Thickness_in_Pigs_Measured_by_Ultrasound_Pachymetry_In_Vivo/links/09509cf5d208dc4a75a25276/Corneal-Thickness-in-Pigs-Measured-by-Ultrasound-Pachymetry-In-Vivo.pdf

120. Suarez T, Vecino E. Expression of endothelial leukocyte adhesion molecule 1 in the aqueous outflow pathway of porcine eyes with induced glaucoma. Mol Vis. 2006;12: 1467–1472. Available: https://www.ncbi.nlm.nih.gov/pubmed/17167401

121. Dang Y, Waxman S, Wang C, Loewen RT, Sun M, Loewen NA. A porcine ex vivo model of pigmentary glaucoma. Sci Rep. 2018;8: 5468. doi:10.1038/s41598-018-23861-x

122. Ruiz-Ederra J, García M, Hernández M, Urcola H, Hernández-Barbáchano E, Araiz J, et al. The pig eye as a novel model of glaucoma. Exp Eye Res. 2005;81: 561–569. doi:10.1016/j.exer.2005.03.014

123. Parikh HA, Loewen RT, Roy P, Schuman JS, Lathrop KL, Loewen NA. Differential Canalograms Detect Outflow Changes from Trabecular Micro-Bypass Stents and Ab

Interno Trabeculectomy. Scientific Reports. 2016. doi:10.1038/srep34705

124. Loewen RT, Brown EN, Scott G, Parikh H, Schuman JS, Loewen NA. Quantification of Focal Outflow Enhancement Using Differential Canalograms. Invest Ophthalmol Vis Sci. 2016;57: 2831–2838. doi:10.1167/iovs.16-19541

125. Hong Y, Wang C, Loewen R, Waxman S, Shah P, Chen S, et al. Outflow facility and extent of angle closure in a porcine model. Graefes Arch Clin Exp Ophthalmol. 2019;257: 1239–1245. doi:10.1007/s00417-019-04279-1

126. Waxman S, Wang C, Dang Y, Hong Y, Esfandiari H, Shah P, et al. Structure-Function Changes of the Porcine Distal Outflow Tract in Response to Nitric Oxide. Invest Ophthalmol Vis Sci. 2018;59: 4886–4895. doi:10.1167/iovs.18-24943

127. Chen S, Waxman S, Wang C, Atta S, Loewen R, Loewen NA. Dose-dependent effects of netarsudil, a Rho-kinase inhibitor, on the distal outflow tract. Graefes Arch Clin Exp Ophthalmol. 2020;258: 1211–1216. doi:10.1007/s00417-020-04691-y

128. Birke MT, Birke K, Lütjen-Drecoll E, Schlötzer-Schrehardt U, Hammer CM. Cytokine-dependent ELAM-1 induction and concomitant intraocular pressure regulation in porcine anterior eye perfusion culture. Invest Ophthalmol Vis Sci. 2011;52: 468–475. doi:10.1167/iovs.10-5990

129. Dang Y, Waxman S, Wang C, Jensen A, Loewen RT, Bilonick RA, et al. Freeze-thaw decellularization of the trabecular meshwork in an ex vivo eye perfusion model. PeerJ. 2017;5: e3629. doi:10.7717/peerj.3629

130. Loewen RT, Brown EN, Roy P, Schuman JS, Sigal IA, Loewen NA. Regionally Discrete Aqueous Humor Outflow Quantification Using Fluorescein Canalograms. PLoS One. 2016;11: e0151754. doi:10.1371/journal.pone.0151754

131. Keller KE, Bhattacharya SK, Borrás T, Brunner TM, Chansangpetch S, Clark AF, et al. Consensus recommendations for trabecular meshwork cell isolation, characterization and culture. Exp Eye Res. 2018;171: 164–173. doi:10.1016/j.exer.2018.03.001

132. Lakowicz JR, editor. Quenching of Fluorescence. Principles of Fluorescence Spectroscopy. Boston, MA: Springer US; 2006. pp. 277–330. doi:10.1007/978-0-387-46312-4_8

133. Parikh HA, Loewen RT, Roy P, Schuman JS, Lathrop KL, Loewen NA. Differential Canalograms Detect Outflow Changes from Trabecular Micro-Bypass Stents and Ab Interno Trabeculectomy. Sci Rep. 2016;6: 34705. doi:10.1038/srep34705

134. Dang Y, Waxman S, Wang C, Parikh HA, Bussel II, Loewen RT, et al. Rapid learning curve assessment in an ex vivo training system for microincisional glaucoma surgery. Sci Rep. 2017;7: 1605. doi:10.1038/s41598-017-01815-z

135. Dang Y, Wang C, Shah P, Waxman S, Loewen RT, Hong Y, et al. Outflow enhancement by three different ab interno trabeculectomy procedures in a porcine anterior segment model. Graefes Arch Clin Exp Ophthalmol. 2018;256: 1305–1312. doi:10.1007/s00417-018-3990-0

136. Loewen RT, Roy P, Parikh HA, Dang Y, Schuman JS, Loewen NA. Impact of a Glaucoma Severity Index on Results of Trabectome Surgery: Larger Pressure Reduction in More Severe Glaucoma. PLoS One. 2016;11: e0151926. doi:10.1371/journal.pone.0151926

137. Katsanos A, Tsaldari N, Gorgoli K, Lalos F, Stefaniotou M, Asproudis I. Safety and Efficacy of YAG Laser Vitreolysis for the Treatment of Vitreous Floaters: An Overview. Adv Ther. 2020;37: 1319–1327. doi:10.1007/s12325-020-01261-w

138. Loewen RT, Waxman S, Wang C, Atta S, Chen S, Watkins SC, et al. 3D-Reconstruction of the human conventional outflow system by ribbon scanning confocal microscopy. PLoS One. 2020;15: e0232833. doi:10.1371/journal.pone.0232833

Appendix

I. List of Abbreviations

AAP	Angular Aqueous Plexus
AH	Aqueous Humor
AIT	Ab Interno Trabeculectomy
ALT	Argon Laser Trabeculoplasty
C	Control Group
DMEM	Dulbecco's Modified Eagle Medium
EVP	Episcleral Venous Pressure
IOP	Intraocular Pressure
KDB	Kahook Dual Blade
MIGS	Microinvasive Glaucoma Surgery
Nd:YAG	Neodymium-Doped Yttrium Aluminum Garnet
NPV	Negative Predictive Value
PBS	Phosphate-Buffered Saline
POAG	Primary Open-Angle Glaucoma
PPV	Positive Predictive Value
RNFL	Retinal Nerve Fiber Layer
ROC	Receiver Operating Characteristics
SC	Schlemm's Canal
SL	Schwalbe's Line
SLT	Selective Laser Trabeculoplasty
T	Trial Group
KDB	Kahook Dual Blade

II. Figures

III. Tables

IV. Acknowledgments

None